Ultrasound
in medicine
and biology

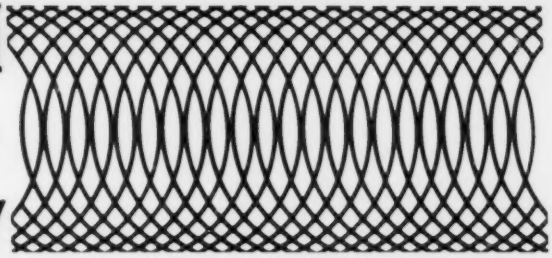

Supplement to *Ultrasound in Medicine and Biology*, Volume 18, Number 5, 1992

Author–Subject Index
Volume 17 (1991)

Compiled by

Michael Halliwell
Department of Medical Physics, Bristol General Hospital, Bristol BS1 6SY, England

PERGAMON PRESS

NEW YORK · OXFORD · SEOUL · TOKYO

ULTRASOUND IN MEDICINE AND BIOLOGY

WORLD FEDERATION FOR ULTRASOUND IN MEDICINE AND BIOLOGY

President: M. FUKUDA, *Sapporo, Japan*
Vice-President: H. TAKEUCHI, *Tokyo, Japan*
Past-President: F. WEILL, *Besançon, France*
President-Elect: B. GOLDBERG, *Philadelphia, U.S.A.*
Treasurer: W. O'BRIEN, *Urbana, U.S.A.*
Secretary: D. ROBINSON, *Chatswood, Australia*
Editor of the Journal: D. N. WHITE, *Kingston, Canada*
Councillors: C. R. B. MERRITT, *New Orleans, U.S.A.*
H. WATANABE, *Kyoto, Japan*
H. LUTZ, *Bayreuth, Germany*
G. CERRI, *São Paulo, Brazil*
W. WIBISONO, *Jakarta, Indonesia*
S. HANCKE, *Hellerup, Denmark*
M. ZISKIN, *Philadelphia, U.S.A.*
S. EIK-NES, *Trondheim, Norway*

AFFILIATED SOCIETIES

American Institute of Ultrasound in Medicine (AIUM), L. Nelson, Secretary, 4405 East-West Highway, Suite 504, Bethesda, MD 20814, U.S.A.

Asian Federation of Societies for Ultrasound in Medicine and Biology (AFSUMB), Dr. H. Watanabe, Secretary, Dept. of Urology, Kyoto Prefectural University of Medicine, Kawaramachi-Hirokoji, Kyoto, Japan 602

Australasian Society for Ultrasound in Medicine (ASUM), Secretariat ASUM, 126 Greville Street, Chatswood, NSW 2067, Australia

Egyptian Society for Ultrasonics (ESU), Dr. Y. Mohran, Secretary, 376 Pyramids Road, Giza, Cairo, Egypt

European Federation of Societies for Ultrasound in Medicine and Biology (EFSUMB), Mrs. Lee Surry, Executive Secretary, The Studio, 43 Bond Street, Ealing, London, WS 5AS, England

Latin-American Federation of Societies of Ultrasound in Medicine and Biology (LAFSUMB), Dr. Giovanni Guido Cerri, Av. Paulista, 491 13.° conj. 132, CEP 01311, São Paulo, Brasil

Mediterrean Society of Ultrasonic Societies (MASU), Dr. F. Weill, Secretary, Centre Hospitalier et Universitaire de Besançon, 2 Place Saint-Jaques, 25030 Besançon Cedex, France

Societas Internationalis pro Diagnostica Ultrasonica in Ophthalmologia (SIDUO), Dr. J. M. Thijssen, Secretary, Universiteitskliniek voor Oogheelkunde, 6500 HB Nijmegen, The Netherlands

South African Medical Ultrasound Society (SAMUS), Dr. M. Jacobson, Secretary SAMUS, Box 93499, Yeoville 2143, Republic of South Africa

Publishing, Advertising, and Subscription Offices: Pergamon Press Inc., 660 White Plains Road, Tarrytown, NY 10591-5153, U.S.A., INTERNET "PPI@PERGAMON.COM"; or Pergamon Press Ltd., Headington Hill Hall, Oxford OX3 0BW, England.

Published 10 per annum. Annual institutional subscription rate (1992): £275.00 (US $515.00). *Two-year institutional rate* (1992/1993): £522.50 (US $978.50). *Personal subscription rate* for those whose library subscribes at the regular rate (1992): £82.00 (US $131.00). Members of the World Federation for Ultrasound in Medicine and Biology may order personal subscriptions at a concessional rate; details of these rates are available upon request. Sterling prices are definitive. US dollar prices are quoted for convenience only, and are subject to exchange rate fluctuation. Prices include postage and insurance and are subject to change without notice. Notify 8 weeks in advance of address change with a copy of the subscription mailing label. Back issues of all previously published volumes, in both hard copy and on microform, are available direct from Pergamon Press. Subscription rates for Japan are available on request.

Copyright © 1992 Pergamon Press Ltd.

The Item-Fee Code for this publication is: 0301-5629/92 $5.00 + .00

It is a condition of publication that manuscripts submitted to this journal have not been published and will not be simultaneously submitted or published elsewhere. By submitting a manuscript, the authors agree that the copyright for their article is transferred to the publisher if and when the article is accepted for publication. The copyright covers the exclusive rights to reproduce and distribute the article, including reprints, photographic reproductions, microform or any other reproductions of similar nature and translations. No part of this publication may be reproduced, stored in a retrieval system or transmitted in any form or by any means, electronic, electrostatic, magnetic tape, mechanical, photocopying, recording or otherwise, without permission in writing from the copyright holder.

Photocopying information for users in the U.S.A. The Item-Fee Code for this publication indicates that authorization to photocopy items for internal or personal use is granted by the copyright holder for libraries and other users registered with the Copyright Clearance Center (CCC) Transactional Reporting Service provided the stated fee for copying, beyond that permitted by Section 107 or 108 of the Unites States Copyright Law, is paid. The appropriate remittance of $5.00 per copy per article is paid directly to the Copyright Clearance Center Inc., 27 Congress Street, Salem, MA 01970.

Permission for other use. The copyright owner's consent does not extend to copying for general distribution, for promotion, for creating new works, or for resale. Specific written permission must be obtained from the publisher for copying. Please contact the Subsidiary Rights Manager, Publishing Services Dept. at either Pergamon Press Ltd. or Pergamon Press Inc.

Ultrasound in Medicine and Biology (ISSN 0301-5629) is published 10 per annum by Pergamon Press. Second-class postage paid at Tarrytown, NY and additional mailing offices. Postmaster: Send address changes to **ULTRASOUND IN MEDICINE AND BIOLOGY**, Pergamon Press Inc., 660 White Plains Road, Tarrytown, NY 10591-5153. Address correction requested.

AUTHOR/SUBJECT INDEX

A

A-mode analysis
angle-dependent backscatter from the arterial wall (de Kroon), 121
echographic differentiation of histological types of intraocular melanoma (Thijssen), 127
the relative contributions of myocardial wall thickness and ischemia to ultrasonic myocardial integrated backscatter during experimental ischemia (Rijsterborgh), 41

Abraham, V., see Margulies, N.
Abraham, V., see Muscarella, L. F.

Absorption
absorption in liver at the focus of an ultrasonic shock wave field (Fry), 65

Accuracy
see errors

Ackerstaff, R. G. A., see Legemate, D. A.

Acoustic microscope
the ultrasonic properties of gastric cancer tissues obtained with a scanning acoustic microscope system (Saijo), 709

Acoustic shadows
phase cancellation: a cause of acoustical shadowing at the edges of curved surfaces in B-mode ultrasound images (Rubin), 85

Acoustic streaming
a new ultrasonic method for fluid property measurements (Dymling), 497

Acoustospectrography
echographic differentiation of histological types of intraocular melanoma (Thijssen), 127

Adaptive estimation
adaptive estimation of the mean frequency of a Doppler signal from short data windows (Herment), 901

Adler, R. S., see Rubin, J. M.

Agar gels
sonoluminescence in water and agar gels during irradiation with 0.75 MHz continuous-wave ultrasound (Daniels), 297

Age
variability of quantitative echographic parameters of the liver: intra- and inter-individual spread, temporal- and age-related effects (Hartman), 857

Aggarwal, K. K., see Jain, S. P.

Aggregation
cyclic changes of blood echogenicity in high-frequency ultrasound (de Kroon), 723

Airborne ultrasound
registration of surface structures using airborne focused ultrasound (Sundström), 513
two-dimensional airborne ultrasound real-time linear array scanner—applied to screening for scoliosis (Mauritzson), 519

Allard, L., Langlois, Y. E., Durand, L.-G., Roederer, G. O., Beaudoin, M., Cloutier, G., Roy, P. and Robillard, P.: computer analysis and pattern recognition of Doppler blood flow spectra for disease classification in the lower limb arteries, 211
Almquist, L.-O., see Holmer, N.-G.
Almquist, L.-O., see Johansson, T.
Almquist, L.-O., see Olsson, L.

Amenorrehea
transvaginal sonography and abnormal ovarian appearance in menstrual cycle disturbances (Pache), 589

Amplitude mode
influence of various instrument settings on the flow information derived from the power mode (Jain), 49

Anatomy
identifying acoustic scattering sources in normal renal parenchyma from the anisotropy in acoustic properties (Insana), 613

Anderson, T., see Pye, S. D.
Andersson, J., see Malcus, P.

Angle-dependent backscatter
angle-dependent backscatter from the arterial wall (de Kroon), 121

Anisotropy
identifying acoustic scattering sources in normal renal parenchyma from the anisotropy in acoustic properties (Insana), 613

Anthropometry
two-dimensional airborne ultrasound real-time linear array scanner—applied to screening for scoliosis (Mauritzson), 519

Antitumor effect
effects of high-energy shock waves combined with biological response modifiers in different human kidney cancer xenografts (Oosterhof), 391

Aorta
aortic diameter pulse waves and blood flow velocity in the small, for gestational age, fetus (Stale), 471
assessment of a potentially noninvasive method for monitoring aortic blood flow in children (Lavandier), 107
change in amplitude distributions of Doppler spectrograms recorded below the aortic valve in patients with a valvular aortic stenosis (Cloutier), 667
spectral analysis criteria in duplex scanning of aortoiliac and femoropopliteal arterial disease (Legemate), 769
waveform pattern recognition—a new semiquantitative method for the analysis of fetal aortic and umbilical artery blood flow velocity recorded by Doppler ultrasound (Malcus), 453

Aortic diameter
aortic diameter pulse waves and blood flow velocity in the small, for gestational age, fetus (Stale), 471
assessment of a potentially noninvasive method for monitoring aortic blood flow in children (Lavandier), 107

Aortic stenosis
change in amplitude distributions of Doppler spectrograms recorded below the aortic valve in patients with a valvular aortic stenosis (Cloutier), 667

Aortoiliac disease
effect of distal occlusions on the assessment of aorto-iliac pathology by analysis of Doppler spectra (Van Asten), 849
spectral analysis criteria in duplex scanning of aortoiliac and femoropopliteal arterial disease (Legemate), 769

Apfel, R. E. and Holland, C. K.: gauging the likelihood of cavitation from short-pulse, low-duty cycle diagnostic ultrasound, 179
Apfel, R. E., see Jiang, P.

Arterial diameter
aortic diameter pulse waves and blood flow velocity in the small, for gestational age, fetus (Stale), 471
calculation of pulse-wave velocity using cross correlation—effects of reflexes in the arterial tree (Benthin), 461

Arterial disease
carotid lesions detected by B-mode ultrasonography in Takayasu's arteritis: "macaroni sign" as an indicator of the disease (Maeda), 695
computer analysis and pattern recognition of Doppler blood flow spectra for disease classification in the lower limb arteries (Allard), 211
effect of distal occlusions on the assessment of aorto-iliac pathology by analysis of Doppler spectra (Van Asten), 849
evaluation of internal carotid artery stenosis by transcranial Doppler ultrasonography and oculopneumoplethysmography (Kelly), 577
measurement of intima-media thickness of common carotid arteries with high-resolution B-mode ultrasonography: inter- and intra-observer variability (Salonen), 225
spectral analysis criteria in duplex scanning of aortoiliac and femoropopliteal arterial disease (Legemate), 769
spectral composition of Doppler signals (Hoeks), 751

Arterial pulsatility
aortic diameter pulse waves and blood flow velocity in the small, for gestational age, fetus (Stale), 471
calculation of pulse-wave velocity using cross correlation—effects of reflexes in the arterial tree (Benthin), 461

Arterial wall
angle-dependent backscatter from the arterial wall (de Kroon), 121
calculation of pulse-wave velocity using cross correlation—effects of reflexes in the arterial tree (Benthin), 461

Artery
an investigation of simulated umbilical artery Doppler waveforms. I. The effect of three physical parameters on the maximum frequency envelope and on pulsatility index (Hoskins), 7
an investigation of simulated umbilical artery Doppler waveforms. II. A comparison of three Doppler waveform quality indices (Hoskins), 23
angle-dependent backscatter from the arterial wall (de Kroon), 121
assessment of a potentially noninvasive method for monitoring aortic blood flow in children (Lavandier), 107
calculation of pulse-wave velocity using cross correlation—effects of reflexes in the arterial tree (Benthin), 461
carotid lesions detected by B-mode ultrasonography in Takayasu's arteritis: "macaroni sign" as an indicator of the disease (Maeda), 695
computer analysis and pattern recognition of Doppler blood flow spectra for disease classification in the lower limb arteries (Allard), 211
continuous-wave and pulsed Doppler studies of the breast: clinical results and effect of transducer frequency (Madjar), 31
duplex Doppler sonography of the umbilical arteries: predictive value in IUGR and correlation with birth weight (Worrell), 207
effect of distal occlusions on the assessment of aorto-iliac pathology by analysis of Doppler spectra (Van Asten), 849
effect of maternal posture on the umbilical artery flow velocity waveform (van Katwijk), 683
evaluation of internal carotid artery stenosis by transcranial Doppler ultrasonography and oculopneumoplethysmography (Kelly), 577
measurement of intima-media thickness of common carotid arteries with high-resolution B-mode ultrasonography: inter- and intra-observer variability (Salonen), 225
spectral analysis criteria in duplex scanning of aortoiliac and femoropopliteal arterial disease (Legemate), 769
spectral composition of Doppler signals (Hoeks), 751
waveform pattern recognition—a new semiquantitative method for the analysis of fetal aortic and umbilical artery blood flow velocity recorded by Doppler ultrasound (Malcus), 453

Artifact
a measurement system for continuous-wave ultrasound fields (Persson), 501
a new ultrasonic method for fluid property measurements (Dymling), 497
calculation of pulse-wave velocity using cross correlation—effects of reflexes in the arterial tree (Benthin), 461
evaluation of Doppler ultrasound for blood perfusion measurements (Eriksson), 445
measurement of blood perfusion in tissue using Doppler ultrasound (Dymling), 433
phase cancellation: a cause of acoustical shadowing at the edges of curved surfaces in B-mode ultrasound images (Rubin), 85
pulse-echo imaging using a nondiffracting beam transducer (Lu), 265
regions in the B-mode image of a cylinder where the location of a point reflector is changed by sound speed variation (Soetanto), 355

Atherosclerosis
computer analysis and pattern recognition of Doppler blood flow spectra for disease classification in the lower limb arteries (Allard), 211

effect of distal occlusions on the assessment of aorto-iliac pathology by analysis of Doppler spectra (Van Asten), 849
measurement of intima-media thickness of common carotid arteries with high-resolution B-mode ultrasonography: inter- and intra-observer variability (Salonen), 225
spectral composition of Doppler signals (Hoeks), 751

Atrioventricular valves
effect of fetal breathing movements on fetal cardiac hemodynamics (van der Mooren), 787

Attenuation
change in amplitude distributions of Doppler spectrograms recorded below the aortic valve in patients with a valvular aortic stenosis (Cloutier), 667
echographic differentiation of histological types of intraocular melanoma (Thijssen), 127
identifying acoustic scattering sources in normal renal parenchyma from the anisotropy in acoustic properties (Insana), 613
in situ exposimetry: the ovarian ultrasound examination (Siddiqi), 257
influence of attenuation on measurements of ultrasonic myocardial integrated backscatter during cardiac cycle (an *in vitro* study) (van der Steen), 869
influence of histochemical preparation on acoustic parameters of liver tissue: a 5-MHz study (van der Steen), 879
measurement of the ultrasonic properties of vascular tissues and blood from 35–65 MHz (Lockwood), 653
prediction of *in situ* exposure to ultrasound: a proposed standard experimental method (Preston), 333
prediction of *in situ* exposure to ultrasound: an acoustical attenuation method (Preston), 317
statistical uncertainty in ultrasonic backscatter and attenuation coefficients determined with a reference phantom (Yao), 187
the ultrasonic properties of gastric cancer tissues obtained with a scanning acoustic microscope system (Saijo), 709
ultrasound properties of liver with and without particulate contrast agents (Tuthill), 231

Autoregressive model
accuracy of velocity and shear rate measurements using pulsed Doppler ultrasound: a comparison of signal analysis techniques (Markou), 803
analysis and classification of secondary sounds from the disintegration of kidney stones with acoustic shock waves (Olsson), 491

Axial scattering
angle-dependent backscatter from the arterial wall (de Kroon), 121

Axon
effect of ultrasound on axonal outgrowth in the sympathetic nervous system of the chick (Yip), 139

Axonal outgrowth
effect of ultrasound on axonal outgrowth in the sympathetic nervous system of the chick (Yip), 139

Azadniv, M., see Miller, M. W.

B

B/A
applications of mixture laws for predicting the compositions of tissue phantoms (Jiang), 829

B-mode
measurement of intima-media thickness of common carotid arteries with high-resolution B-mode ultrasonography: inter- and intra-observer variability (Salonen), 225

Backscatter
angle-dependent backscatter from the arterial wall (de Kroon), 121
change in amplitude distributions of Doppler spectrograms recorded below the aortic valve in patients with a valvular aortic stenosis (Cloutier), 667
cyclic changes of blood echogenicity in high-frequency ultrasound (de Kroon), 723
echographic differentiation of histological types of intraocular melanoma (Thijssen), 127
identifying acoustic scattering sources in normal renal parenchyma from the anisotropy in acoustic properties (Insana), 613
influence of attenuation on measurements of ultrasonic myocardial integrated backscatter during cardiac cycle (an *in vitro* study) (van der Steen), 869
influence of histochemical preparation on acoustic parameters of liver tissue: a 5-MHz study (van der Steen), 879
measurement of the ultrasonic properties of vascular tissues and blood from 35–65 MHz (Lockwood), 653
statistical uncertainty in ultrasonic backscatter and attenuation coefficients determined with a reference phantom (Yao), 187
the relative contributions of myocardial wall thickness and ischemia to ultrasonic myocardial integrated backscatter during experimental ischemia (Rijsterborgh), 41
ultrasound properties of liver with and without particulate contrast agents (Tuthill), 231
variability of quantitative echographic parameters of the liver: intra- and inter-individual spread, temporal- and age-related effects (Hartman), 857

Baggs, R. B., see Tuthill, P. A.
Balcer-Kubiczek, E. K., see Harrison, G. H.
Bamber, J. C., see Hill, C. R.
Basset, O., Gimenez, G., Mestas, J. L., Cathignol, D. and Devonec, M.: volume measurement by ultrasonic transverse or sagittal cross-sectional scanning, 291

Beam computation
theoretical predictions of the acoustic pressure generated by a shock wave lithotripter (Coleman), 245

Beam cross-section
a measurement system for continuous-wave ultrasound fields (Persson), 501
measurements of ultrasonic fields with optical diffraction tomography (Holm), 505

Beam distortion
ultimate limits in ultrasonic imaging resolution (Harris), 547

Beam measurement
a measurement system for continuous-wave ultrasound fields (Persson), 501
measurements of ultrasonic fields with optical diffraction tomography (Holm), 505

Beam profile
a measurement system for continuous-wave ultrasound fields (Persson), 501
measurements of ultrasonic fields with optical diffraction tomography (Holm), 505
pulse-echo imaging using a nondiffracting beam transducer (Lu), 265
theoretical predictions of the acoustic pressure generated by a shock wave lithotripter (Coleman), 245
ultimate limits in ultrasonic imaging resolution (Harris), 547

Beaudoin, M., see Allard, L.
Beijneveld, W. J., see Van Asten, W. N. J. C.
Benoni, G., see Mauritzson, L.
Benthin, M., see Stale, H.
Benthin, M., Dahl, P., Ruzicka, R. and Lindström, K.: calculation of pulse-wave velocity using cross-correlation—effects of reflexes in the arterial tree, 461
Berson, M., see Tranquart, F.

Bessel beam
pulse-echo imaging using a nondiffracting beam transducer (Lu), 265

Biliary lithotripsy
ultrasound properties of liver with and without particulate contrast agents (Tuthill), 231

Biliary mucus
ultrasound properties of liver with and without particulate contrast agents (Tuthill), 231

Bioeffects
absence of mutagenic effects of continuous and pulsed ultrasound in cultured (A_L) human-hamster hybrid cells (Ritenour), 921
analysis and classification of secondary sounds from the disintegration of kidney stones with acoustic shock waves (Olsson), 491
early metabolic response to high-energy shock waves in a human tumor kidney xenograft monitored by ^{31}P magnetic resonance spectroscopy (Smits), 791
effect of ultrasound on axonal outgrowth in the sympathetic nervous system of the chick (Yip), 139
effect of ultrasound on regional blood flow in neonatal rats (Muscarella), 893
effects of high-energy shock waves combined with biological response modifiers in different human kidney cancer xenografts (Oosterhof), 391
gauging the likelihood of cavitation from short-pulse, low-duty cycle diagnostic ultrasound (Apfel), 179
in utero measurement of ultrasonically induced fetal mouse temperature increases (Carnes), 373
influence of water conductivity on the efficacy and the reproducibility of electrohydraulic shock wave generation (Cathignol), 819
mechanisms for hemolysis by ultrasonic cavitation in the rotating exposure system (Miller), 171

on the mechanism of kidney stone disintegration by acoustic shock waves (Holmer), 479
pulsed ultrasound and the hyperbarically exposed mouse fetus (Child), 367
reversible biochemical changes in the developing rat central nervous system following ultrasound exposure (Margulies), 383
single strand breaks in CHO cell DNA induced by ultrasonic cavitation *in vitro* (Miller), 401
the threshold for thermally significant cavitation in dog's thigh muscle *in vivo* (Hynynen), 157
thresholds for premature ventricular contractions in frog hearts exposed to lithotripter fields (Dalecki), 341
ultrasound effects on cell proliferation and migration of chick motoneurons (Yip), 55

Biological response modifiers
effects of high-energy shock waves combined with biological response modifiers in different human kidney cancer xenografts (Oosterhof), 391

Birer, A., see Lavandier, B.

Birth weight
duplex Doppler sonography of the umbilical arteries: predictive value in IUGR and correlation with birth weight (Worrell), 207

Blood
cyclic changes of blood echogenicity in high-frequency ultrasound (de Kroon), 723
measurement of the ultrasonic properties of vascular tissues and blood from 35–65 MHz (Lockwood), 653

Blood flow
an investigation of simulated umbilical artery Doppler waveforms. I. The effect of three physical parameters on the maximum frequency envelope and on pulsatility index (Hoskins), 7
an investigation of simulated umbilical artery Doppler waveforms. II. A comparison of three Doppler waveform quality indices (Hoskins), 23
assessment of a potentially noninvasive method for monitoring aortic blood flow in children (Lavandier), 107
carotid lesions detected by B-mode ultrasonography in Takayasu's arteritis: "macaroni sign" as an indicator of the disease (Maeda), 695
change in amplitude distributions of Doppler spectrograms recorded below the aortic valve in patients with a valvular aortic stenosis (Cloutier), 667
comparison of four different Doppler instruments used to measure linear and volumetric cardiac output: a study of reproducibility and agreement (Mayo), 347
computer analysis and pattern recognition of Doppler blood flow spectra for disease classification in the lower limb arteries (Allard), 211
continuous-wave and pulsed Doppler studies of the breast: clinical results and effect of transducer frequency (Madjar), 31
duplex Doppler sonography of the umbilical arteries: predictive value in IUGR and correlation with birth weight (Worrell), 207
effect of distal occlusions on the assessment of aorto-iliac pathology by analysis of Doppler spectra (Van Asten), 849
effect of fetal breathing movements on fetal cardiac hemodynamics (van der Mooren), 787

effect of maternal posture on the umbilical artery flow velocity waveform (van Katwijk), 683
effect of ultrasound on regional blood flow in neonatal rats (Muscarella), 893
evaluation of cerebral blood flow in rabbits with transcranial Doppler sonography: first results (Tranquart), 815
evaluation of Doppler ultrasound for blood perfusion measurements (Eriksson), 445
flow velocity waveforms in the fetal inferior vena cava during the second half of normal pregnancy (Huisman), 679
measurement of blood perfusion in tissue using Doppler ultrasound (Dymling), 433
nonstationarity broadening in pulsed Doppler spectrum measurements (Fish), 147
spectral analysis criteria in duplex scanning of aortoiliac and femoropopliteal arterial disease (Legemate), 769
spectral composition of Doppler signals (Hoeks), 751
waveform pattern recognition—a new semiquantitative method for the analysis of fetal aortic and umbilical artery blood flow velocity recorded by Doppler ultrasound (Malcus), 453

Blood perfusion
effect of ultrasound on regional blood flow in neonatal rats (Muscarella), 893
evaluation of Doppler ultrasound for blood perfusion measurements (Eriksson), 445
measurement of blood perfusion in tissue using Doppler ultrasound (Dymling), 433

Blood pressure
aortic diameter pulse waves and blood flow velocity in the small, for gestational age, fetus (Stale), 471

Blood velocity
adaptive estimation of the mean frequency of a Doppler signal from short data windows (Herment), 901
aortic diameter pulse waves and blood flow velocity in the small, for gestational age, fetus (Stale), 471
assessment of a potentially noninvasive method for monitoring aortic blood flow in children (Lavandier), 107
effect of distal occlusions on the assessment of aorto-iliac pathology by analysis of Doppler spectra (Van Asten), 849
effect of fetal breathing movements on fetal cardiac hemodynamics (van der Mooren), 787
evaluation of cerebral blood flow in rabbits with transcranial Doppler sonography: first results (Tranquart), 815
nonstationarity broadening in pulsed Doppler spectrum measurements (Fish), 147
spectral analysis criteria in duplex scanning of aortoiliac and femoropopliteal arterial disease (Legemate), 769
spectral composition of Doppler signals (Hoeks), 751
waveform pattern recognition—a new semiquantitative method for the analysis of fetal aortic and umbilical artery blood flow velocity recorded by Doppler ultrasound (Malcus), 453

Bodard, S., see Tranquart, F.
Bom, N., see de Kroon, M. G. M.

Bom, N., see de Kroon, M. G. M.
Bom, N., see Rijsterborgh, H.
Bom, N., see van der Steen, A. F. W.
Börjesson, P. O., see Sundström, N.
Bosman, G., Reuss, A., Nijman, J. M. and Wladimiroff, J. W.: prenatal diagnosis, management and outcome of fetal uretero-pelvic junction obstruction, 117
Braaton, M., see Ritenour, E. R.
Bräunlich, M., see Sass, W.

Breast
continuous-wave and pulsed Doppler studies of the breast: clinical results and effect of transducer frequency (Madjar), 31

Brümmer, F., see Suhr, D.

Bubble detection
the use of frequency mixing to distinguish size distributions of gas-filled micropores (Quain), 71

Bubble growth
gauging the likelihood of cavitation from short-pulse, low-duty cycle diagnostic ultrasound (Apfel), 179
sonoluminescence in water and agar gels during irradiation with 0.75 MHz continuous-wave ultrasound (Daniels), 297

Bubble resonance
gauging the likelihood of cavitation from short-pulse, low-duty cycle diagnostic ultrasound (Apfel), 179
sonoluminescence in water and agar gels during irradiation with 0.75 MHz continuous-wave ultrasound (Daniels), 297
the use of frequency mixing to distinguish size distributions of gas-filled micropores (Quain), 71

C

Cancellation, phase
phase cancellation: a cause of acoustical shadowing at the edges of curved surfaces in B-mode ultrasound images (Rubin), 85

Capriotti, C., see Yip, Y. P.
Capriotti, C., see Yip, Y. P. L.

Cardiac cycle
cyclic changes of blood echogenicity in high-frequency ultrasound (de Kroon), 723
influence of attenuation on measurements of ultrasonic myocardial integrated backscatter during cardiac cycle (an *in vitro* study) (van der Steen), 869

Cardiac effects
thresholds for premature ventricular contractions in frog hearts exposed to lithotripter fields (Dalecki), 341

Cardiac outflow tracts
effect of fetal breathing movements on fetal cardiac hemodynamics (van der Mooren), 787

Cardiac output
comparison of four different Doppler instruments used to measure linear and volumetric cardiac output: a study of reproducibility and agreement (Mayo), 347

Cardiology
the relative contributions of myocardial wall thickness and ischemia to ultrasonic myocardial integrated backscatter during experimental ischemia (Rijsterborgh), 41

Carnes, K. I., Drewniak, J. L. and Dunn, F.: *in utero* measurement of ultrasonically induced fetal mouse temperature increases, 373

Carotid artery
carotid lesions detected by B-mode ultrasonography in Takayasu's arteritis: "macaroni sign" as an indicator of the disease (Maeda), 695
evaluation of internal carotid artery stenosis by transcranial Doppler ultrasonography and oculopneumoplethysmography (Kelly), 577
measurement of intima-media thickness of common carotid arteries with high-resolution B-mode ultrasonography: inter- and intra-observer variability (Salonen), 225
measurement of the ultrasonic properties of vascular tissues and blood from 35–65 MHz (Lockwood), 653

Carson, P. L., see Rubin, J. M.
Carstensen, E. L., see Child, S. Z.
Carstensen, E. L., see Dalecki, D.

Catalase
cavitation-generated free radicals during shock wave exposure: investigation with cell-free solutions and suspended cells (Suhr), 761

Cathignol, D., Mestas, J. L., Gomez, F. and Lenz, P.: influence of water conductivity on the efficacy and the reproducibility of electrohydraulic shock wave generation, 819
Cathignol, D., see Basset, O.
Cathignol, D., see Lavandier, B.

Cavitation
cavitation-generated free radicals during shock wave exposure: investigation with cell-free solutions and suspended cells (Suhr), 761
gauging the likelihood of cavitation from short-pulse, low-duty cycle diagnostic ultrasound (Apfel), 179
mechanisms for hemolysis by ultrasonic cavitation in the rotating exposure system (Miller), 171
on the mechanism of kidney stone disintegration by acoustic shock waves (Holmer), 479
pulsed ultrasound and the hyperbarically exposed mouse fetus (Child), 367
single strand breaks in CHO cell DNA induced by ultraso[illegible]cavitation *in vitro* (Miller), 401
sonoluminescence in water and agar gels during irradiation with 0.75 MHz continuous-wave ultrasound (Daniels), 297
the mechanisms of stone disintegration by shock waves (Sass), 239
the threshold for thermally significant cavitation in dog's thigh muscle *in vivo* (Hynynen), 157

the use of frequency mixing to distinguish size distributions of gas-filled microspores (Quain), 71
ultrasonic cavitation indirectly induces single strand breaks in DNA of viable cells *in vitro* by the action of residual hydrogen peroxide (Miller), 729

Cell migration
ultrasound effects on cell proliferation and migration of chick motoneurons (Yip), 55

Cells
absence of mutagenic effects of continuous and pulsed ultrasound in cultured (A_L) human-hamster hybrid cells (Ritenour), 921
cavitation-generated free radicals during shock wave exposure: investigation with cell-free solutions and suspended cells (Suhr), 761
synergism between hyperthermia, ultrasound and gamma irradiation (Loverock), 607
ultrasound effects on cell proliferation and migration of chick motoneurons (Yip), 55

Central nervous system
reversible biochemical changes in the developing rat central nervous system following ultrasound exposure (Margulies), 383

Cerebral artery
evaluation of cerebral blood flow in rabbits with transcranial Doppler sonography: first results (Tranquart), 815

Cerebral blood flow
effect of ultrasound on regional blood flow in neonatal rats (Muscarella), 893

Chang, J. Y., see Kelly, R. E.
Chen, C. F., see Robinson, D. E.

Chick embryos
effect of ultrasound on axonal outgrowth in the sympathetic nervous system of the chick (Yip), 139
ultrasound effects on cell proliferation and migration of chick motoneurons (Yip), 55

Chignier, E., see Lavandier, B.
Child, S. Z., Hoffman, D., Norton, S., Carstensen, E. L., Cox, C. and Gates, A. H.: pulsed ultrasound and the hyperbarically exposed mouse fetus, 367

Children
assessment of a potentially noninvasive method for monitoring aortic blood flow in children (Lavandier), 107

Chinese hamster ovary
single strand breaks in CHO cell DNA induced by ultrasonic cavitation *in vitro* (Miller), 401

Choi, M. J., see Coleman, A. J.

Choroidal melanoma
echographic differentiation of histological types of intraocular melanoma (Thijssen), 127

Chromosomes
lack of induced increase in sister chromatid exchanges in human lymphocytes exposed to *in vivo* therapeutic ultrasound (Miller), 81

Chronic hydrocephalus
evaluation of cerebral blood flow in rabbits with transcranial Doppler sonography: first results (Tranquart), 815

Circadian rhythm
variability of quantitative echographic parameters of the liver: intra- and inter-individual spread, temporal- and age-related effects (Hartman), 857

Clinical evaluation
clinical trial of umbilical artery Doppler waveform quality indices (Hoskins), 777
comparison of four different Doppler instruments used to measure linear and volumetric cardiac output: a study of reproducibility and agreement (Mayo), 347
continuous-wave and pulsed Doppler studies of the breast: clinical results and effect of transducer frequency (Madjar), 31
echographic differentiation of histological types of intraocular melanoma (Thijssen), 127
waveform pattern recognition—a new semiquantitative method for the analysis of fetal aortic and umbilical artery blood flow velocity recorded by Doppler ultrasound (Malcus), 453

Cloutier, G., see Allard, L.
Cloutier, G., Lemire, F., Durand, L.-G., Latour, Y., Jarry, M., Solignac, A. and Langlois, Y. E.: change in amplitude distributions of Doppler spectrograms recorded below the aortic valve in patients with a valvular aortic stenosis, 667
Cobbold, R. S. C., see Tamura, T.

Cocarcinogenesis
pulsed ultrasound and neoplastic transformation *in vitro* (Harrison), 627

Coleman, A. J., Choi, M. J. and Saunders, J. E.: theoretical predictions of the acoustic pressure generated by a shock wave lithotripter, 245

Color Doppler hard copy
the use of ink jets in ultrasound registrations (Johansson), 529

Color flow
adaptive estimation of the mean frequency of a Doppler signal from short data windows (Herment), 901
continuous-wave and pulsed Doppler studies of the breast: clinical results and effect of transducer frequency (Madjar), 31
influence of various instrument settings on the flow information derived from the power mode (Jain), 49
quantitative study of steady flow using color Doppler ultrasound (Tamura), 595

Complex flow
quantitative study of steady flow using color Doppler ultrasound (Tamura), 595

Compliance
aortic diameter pulse waves and blood flow velocity in the small, for gestational age, fetus (Stale), 471
calculation of pulse-wave velocity using cross correlation—effects of reflexes in the arterial tree (Benthin), 461

Compressibility
applications of mixture laws for predicting the compositions of tissue phantoms (Jiang), 829

Conductivity, water
influence of water conductivity on the efficacy and the reproducibility of electrohydraulic shock wave generation (Cathignol), 819

Continuous ink jet printer
the use of ink jets in ultrasound registrations (Johansson), 529

Continuous-wave Doppler
an investigation of simulated umbilical artery Doppler waveforms. I. The effect of three physical parameters on the maximum frequency envelope and on pulsatility index (Hoskins), 7
an investigation of simulated umbilical artery Doppler waveforms. II. A comparison of three Doppler waveform quality indices (Hoskins), 23
clinical trial of umbilical artery Doppler waveform quality indices (Hoskins), 777
comparison of four different Doppler instruments used to measure linear and volumetric cardiac output: a study of reproducibility and agreement (Mayo), 347
continuous-wave and pulsed Doppler studies of the breast: clinical results and effect of transducer frequency (Madjar), 31
evaluation of Doppler ultrasound for blood perfusion measurements (Eriksson), 445
measurement of blood perfusion in tissue using Doppler ultrasound (Dymling), 433
spectral composition of Doppler signals (Hoeks), 751

Contour measurement
registration of surface structures using airborne focused ultrasound (Sundström), 513

Contrast resolution
ultimate limits in ultrasonic imaging resolution (Harris), 547
what might echography learn from imaging science? (Hill), 559

Correlation
adaptive estimation of the mean frequency of a Doppler signal from short data windows (Herment), 901
calculation of pulse-wave velocity using cross correlation—effects of reflexes in the arterial tree (Benthin), 461
comparison of four different Doppler instruments used to measure linear and volumetric cardiac output: a study of reproducibility and agreement (Mayo), 347
echographic differentiation of histological types of intraocular melanoma (Thijssen), 127

identifying acoustic scattering sources in normal renal parenchyma from the anisotropy in acoustic properties (Insana), 613

Cox, C., see Child, S. Z.
Cox, C., see Miller, M. W.
Crawford, D. C., see Hill, C. R.

Curved target
phase cancellation: a cause of acoustical shadowing at the edges of curved surfaces in B-mode ultrasound images (Rubin), 85

Cuypers, M. H. M., see van der Steen, A. F. W.

Cyclic changes
cyclic changes of blood echogenicity in high-frequency ultrasound (de Kroon), 723
influence of attenuation on measurements of ultrasonic myocardial integrated backscatter during cardiac cycle (an *in vitro* study) (van der Steen), 869
variability of quantitative echographic parameters of the liver: intra- and inter-individual spread, temporal- and age-related effects (Hartman), 857

Cystic kidney disease
sonographic, clinical and genetic aspects of prenatal diagnosis of cystic kidney disease (Reuss), 687

Cytotoxicity
absence of mutagenic effects of continuous and pulsed ultrasound in cultured (A_L) human-hamster hybrid cells (Ritenour), 921

D

Dahl, P., see Benthin, M.
Dahl, P., see Stale, H.
Dalecki, D., Keller, B. B., Carstensen, E. L., Neel, D. S., Palladino, J. L. and Noordergraaf, A.: thresholds for premature ventricular contractions in frog hearts exposed to lithotripter fields, 341
Daniels, S. and Price, D. J.: sonoluminescence in water and agar gels during irradiation with 0.75 MHz continuous-wave ultrasound, 297
Debruyne, F. M. J., see Oosterhof, G. O. N.
Debruyne, F. M. J., see Smits, G. A. H. J.
Demoment, G., see Herment, A.

Density
applications of mixture laws for predicting the compositions of tissue phantoms (Jiang), 829

Descending thoracic aorta
assessment of a potentially noninvasive method for monitoring aortic blood flow in children (Lavandier), 107

Devonec, M., see Basset, O.

Difference frequency
the use of frequency mixing to distinguish size distributions of gas-filled micropores (Quain), 71

Digital subtraction angiography
spectral analysis criteria in duplex scanning of aortoiliac and femoropopliteal arterial disease (Legemate), 769

Dines, D. A., see Fry, F. J.

Discrimination
ultimate limits in ultrasonic imaging resolution (Harris), 547
what might echography learn from imaging science? (Hill), 559

Distal occlusion
effect of distal occlusions on the assessment of aorto-iliac pathology by analysis of Doppler spectra (Van Asten), 849

Distortion
regions in the B-mode image of a cylinder where the location of a point reflector is changed by sound speed variation (Soetanto), 355
ultimate limits in ultrasonic imaging resolution (Harris), 547

DNA strand breaks
single strand breaks in CHO cell DNA induced by ultrasonic cavitation *in vitro* (Miller), 401
ultrasonic cavitation indirectly induces single strand breaks in DNA of viable cells *in vitro* by the action of residual hydrogen peroxide (Miller), 729

Dog
mechanisms for hemolysis by ultrasonic cavitation in the rotating exposure system (Miller), 171
the threshold for thermally significant cavitation in dog's thigh muscle *in vivo* (Hynynen), 157

Doppler
a new ultrasonic method for fluid property measurements (Dymling), 497
accuracy of velocity and shear rate measurements using pulsed Doppler ultrasound: a comparison of signal analysis techniques (Markou), 803
adaptive estimation of the mean frequency of a Doppler signal from short data windows (Herment), 901
an investigation of simulated umbilical artery Doppler waveforms. I. The effect of three physical parameters on the maximum frequency envelope and on pulsatility index (Hoskins), 7
an investigation of simulated umbilical artery Doppler waveforms. II. A comparison of three Doppler waveform quality indices (Hoskins), 23
an investigation of simulated umbilical artery Doppler waveforms. III. The effect of noise reduction algorithms on the maximum frequency envelope and on the pulsatility index (Hoskins), 703
assessment of a potentially noninvasive method for monitoring aortic blood flow in children (Lavandier), 107
author's reply to "velocity estimation using duplex scanners," 195L (Tessler), 199L
change in amplitude distributions of Doppler spectrograms recorded below the aortic valve in patients with a valvular aortic stenosis (Cloutier), 667
clinical trial of umbilical artery Doppler waveform quality indices (Hoskins), 777
comparison of four different Doppler instruments used to measure linear and volumetric cardiac output: a study of reproducibility and agreement (Mayo), 347

computer analysis and pattern recognition of Doppler blood flow spectra for disease classification in the lower limb arteries (Allard), 211
continuous-wave and pulsed Doppler studies of the breast: clinical results and effect of transducer frequency (Madjar), 31
duplex Doppler sonography of the umbilical arteries: predictive value in IUGR and correlation with birth weight (Worrell), 207
effect of distal occlusions on the assessment of aorto-iliac pathology by analysis of Doppler spectra (Van Asten), 849
effect of fetal breathing movements on fetal cardiac hemodynamics (van der Mooren), 787
effect of maternal posture on the umbilical artery flow velocity waveform (van Katwijk), 683
evaluation of cerebral blood flow in rabbits with transcranial Doppler sonography: first results (Tranquart), 815
evaluation of Doppler ultrasound for blood perfusion measurements (Eriksson), 445
evaluation of internal carotid artery stenosis by transcranial Doppler ultrasonography and oculopneumoplethysmography (Kelly), 577
flow velocity waveforms in the fetal inferior vena cava during the second half of normal pregnancy (Huisman), 679
influence of various instrument settings on the flow information derived from the power mode (Jain), 49
measurement of blood perfusion in tissue using Doppler ultrasound (Dymling), 433
nonstationarity broadening in pulsed Doppler spectrum measurements (Fish), 147
quantitative study of steady flow using color Doppler ultrasound (Tamura), 595
spectral analysis criteria in duplex scanning of aortoiliac and femoropopliteal arterial disease (Legemate), 769
spectral composition of Doppler signals (Hoeks), 751
velocity estimation using duplex scanners (Hoskins), 195L

Doppler angle
an investigation of simulated umbilical artery Doppler waveforms. I. The effect of three physical parameters on the maximum frequency envelope and on pulsatility index (Hoskins), 7
assessment of a potentially noninvasive method for monitoring aortic blood flow in children (Lavandier), 107

Doppler equation
an investigation of simulated umbilical artery Doppler waveforms. I. The effect of three physical parameters on the maximum frequency envelope and on pulsatility index (Hoskins), 7
accuracy of velocity and shear rate measurements using pulsed Doppler ultrasound: a comparison of signal analysis techniques (Markou), 803
assessment of a potentially noninvasive method for monitoring aortic blood flow in children (Lavandier), 107
spectral composition of Doppler signals (Hoeks), 751

Doppler power spectrum
nonstationarity broadening in pulsed Doppler spectrum measurements (Fish), 147

Dosimetry
in situ exposimetry: the ovarian ultrasound examination (Siddiqi), 257

Doubling time
effects of high-energy shock waves combined with biological response modifiers in different human kidney cancer xenografts (Oosterhof), 391

Drewniak, J. L., see Carnes, K. I.
Dreyer, H.-P., see Sass, W.
Drolshagen, L. F., see Worrell, J. A.

Ductus venosus
flow velocity waveforms in the fetal inferior vena cava during the second half of normal pregnancy (Huisman), 679

Dumee, Ph., see Herment, A.
Dunn, F., see Carnes, K. I.
Dunn, F., see Saijo, Y.

Duplex scanner
author's reply to "velocity estimation using duplex scanners," 195L (Tessler), 199L
continuous-wave and pulsed Doppler studies of the breast: clinical results and effect of transducer frequency (Madjar), 31
duplex Doppler sonography of the umbilical arteries: predictive value in IUGR and correlation with birth weight (Worrell), 207
spectral analysis criteria in duplex scanning of aortoiliac and femoropopliteal arterial disease (Legemate), 769
velocity estimation using duplex scanners (Hoskins), 195L

Durand, L.-G., see Allard, L.
Durand, L.-G., see Cloutier, G.
Durmon, G. R., see Worrell, J. A.
Dymling, S. O., see Eriksson, R.
Dymling, S. O., see Persson, H. W.
Dymling, S. O., Persson, H. W. and Hertz, C. H.: measurement of blood perfusion in tissue using Doppler ultrasound, 433
Dymling, S. O., Persson, H. W., Hertz, T. G. and Lindström, K.: a new ultrasonic method for fluid property measurements, 497

Dynamic focusing
pulse-echo imaging using a nondiffracting beam transducer (Lu), 265

E

Echographic analysis
echographic differentiation of histological types of intraocular melanoma (Thijssen), 127
variability of quantitative echographic parameters of the liver: intra- and inter-individual spread, temporal- and age-related effects (Hartman), 857

Echographic density
echographic differentiation of histological types of intraocular melanoma (Thijssen), 127
variability of quantitative echographic parameters of the liver: intra- and inter-individual spread, temporal- and age-related effects (Hartman), 857

Echo texture
echographic differentiation of histological types of intraocular melanoma (Thijssen), 127

Echo tracking
aortic diameter pulse waves and blood flow velocity in the small, for gestational age, fetus (Stale), 471
calculation of pulse-wave velocity using cross correlation—effects of reflexes in the arterial tree (Benthin), 461

Edge shadow artifact
phase cancellation: a cause of acoustical shadowing at the edges of curved surfaces in B-mode ultrasound images (Rubin), 85

Eikelboom, B. C., see Legemate, D. A.
Edler, I.: early echocardiography, 425

Elasticity
aortic diameter pulse waves and blood flow velocity in the small, for gestational age, fetus (Stale), 471
calculation of pulse-wave velocity using cross correlation—effects of reflexes in the arterial tree (Benthin), 461

Electromagnetic flowmeter
assessment of a potentially noninvasive method for monitoring aortic blood flow in children (Lavandier), 107

Embryo
aortic diameter pulse waves and blood flow velocity in the small, for gestational age, fetus (Stale), 471
duplex Doppler sonography of the umbilical arteries: predictive value in IUGR and correlation with birth weight (Worrell), 207
effect of fetal breathing movements on fetal cardiac hemodynamics (van der Mooren), 787
flow velocity waveforms in the fetal inferior vena cava during the second half of normal pregnancy (Huisman), 679
in utero measurement of ultrasonically induced fetal mouse temperature increases (Carnes), 373
prenatal diagnosis, management and outcome of fetal uretero-pelvic junction obstruction (Bosman), 117
pulsed ultrasound and neoplastic transformation *in vitro* (Harrison), 627
pulsed ultrasound and the hyperbarically exposed mouse fetus (Child), 367
reversible biochemical changes in the developing rat central nervous system following ultrasound exposure (Margulies), 383
sonographic, clinical and genetic aspects of prenatal diagnosis of cystic kidney disease (Reuss), 687
waveform pattern recognition—a new semiquantitative method for the analysis of fetal aortic and umbilical artery blood flow velocity recorded by Doppler ultrasound (Malcus), 453

Endoscopic ultrasonography
cyclic changes of blood echogenicity in high-frequency ultrasound (de Kroon), 723
the ultrasonic properties of gastric cancer tissues obtained with a scanning acoustic microscope system (Saijo), 709

Eriksson, R., Persson, H. W., Dymling, S. O. and Lindström, K.: evaluation of Doppler ultrasound for blood perfusion measurements, 445

Errors
accuracy of velocity and shear rate measurements using pulsed Doppler ultrasound: a comparison of signal analysis techniques (Markou), 803
an investigation of simulated umbilical artery Doppler waveforms. I. The effect of three physical parameters on the maximum frequency envelope and on pulsatility index (Hoskins), 7
an investigation of simulated umbilical artery Doppler waveforms. II. A comparison of three Doppler waveform quality indices (Hoskins), 23
an investigation of simulated umbilical artery Doppler waveforms. III. The effect of noise reduction algorithms on the maximum frequency envelope and on the pulsatility index (Hoskins), 703
author's reply to "velocity estimation using duplex scanners," 195L (Tessler), 199L
calculation of pulse-wave velocity using cross correlation—effects of reflexes in the arterial tree (Benthin), 461
comparison of four different Doppler instruments used to measure linear and volumetric cardiac output: a study of reproducibility and agreement (Mayo), 347
evaluation of Doppler ultrasound for blood perfusion measurements (Eriksson), 445
incorrect description of an ultrasonic beam (Kremkau), 411L
influence of various instrument settings on the flow information derived from the power mode (Jain), 49
measurement of blood perfusion in tissue using Doppler ultrasound (Dymling), 433
measurement of intima-media thickness of common carotid arteries with high-resolution B-mode ultrasonography: inter- and intra-observer variability (Salonen), 225
nonstationarity broadening in pulsed Doppler spectrum measurements (Fish), 147
pulse-echo ultrasound speed measurements: progress and prospects (Robinson), 633
quantitative study of steady flow using color Doppler ultrasound (Tamura), 595
regions in the B-mode image of a cylinder where the location of a point reflector is changed by sound speed variation (Soetanto), 355
spectral composition of Doppler signals (Hoeks), 751
statistical uncertainty in ultrasonic backscatter and attenuation coefficients determined with a reference phantom (Yao), 187
velocity estimation using duplex scanners (Hoskins), 195L
volume measurement by ultrasonic transverse or sagittal cross-sectional scanning (Basset), 291

Erythrocyte aggregation
cyclic changes of blood echogenicity in high-frequency ultrasound (de Kroon), 723

Esophageal scanning
assessment of a potentially noninvasive method for monitoring aortic blood flow in children (Lavandier), 107

Etchison, M. R., see Fry, F. J.
Everbach, E. C., see Jiang, P.

Exposimetry
in situ exposimetry: the ovarian ultrasound examination (Siddiqi), 257
prediction of *in situ* exposure to ultrasound: a proposed standard experimental method (Preston), 333
prediction of *in situ* exposure to ultrasound: an acoustical attenuation method (Preston), 317

Exposure
in situ exposimetry: the ovarian ultrasound examination (Siddiqi), 257
prediction of *in situ* exposure to ultrasound: a proposed standard experimental method (Preston), 333
prediction of *in situ* exposure to ultrasound: an acoustical attenuation method (Preston), 317

Extracorporeal Shock Wave Lithotripsy (ESWL)
analysis and classification of secondary sounds from the disintegration of kidney stones with acoustic shock waves (Olsson), 491
cavitation-generated free radicals during shock wave exposure: investigation with cell-free solutions and suspended cells (Suhr), 761
combined reflection and transmission ultrasound imaging (Green), 283
early metabolic response to high-energy shock waves in a human tumor kidney xenograft monitored by ^{31}P magnetic resonance spectroscopy (Smits), 791
effects of high-energy shock waves combined with biological response modifiers in different human kidney cancer xenografts (Oosterhof), 391
estimation of transient temperature elevation in lithotripsy and in ultrasonography (Filipczynski), 715
influence of water conductivity on the efficacy and the reproducibility of electrohydraulic shock wave generation (Cathignol), 819
on the mechanism of kidney stone disintegration by acoustic shock waves (Holmer), 479
robust electromagnetic probe for the monitoring of lithotriptor output (Pye), 931
the mechanisms of stone disintegration by shock waves (Sass), 239
theoretical predictions of the acoustic pressure generated by a shock wave lithotripter (Coleman), 245
thresholds for premature ventricular contractions in frog hearts exposed to lithotripter fields (Dalecki), 341

Extracorporeal shock waves
analysis and classification of secondary sounds from the disintegration of kidney stones with acoustic shock waves (Olsson), 491
effects of high-energy shock waves combined with biological response modifiers in different human kidney cancer xenografts (Oosterhof), 391
estimation of transient temperature elevation in lithotripsy and in ultrasonography (Filipczynski), 715
influence of water conductivity on the efficacy and the reproducibility of electrohydraulic shock wave generation (Cathignol), 819
on the mechanism of kidney stone disintegration by acoustic shock waves (Holmer), 479

robust electromagnetic probe for the monitoring of lithotriptor output (Pye), 931
the mechanisms of stone disintegration by shock waves (Sass), 239
theoretical predictions of the acoustic pressure generated by a shock wave lithotripter (Coleman), 245
thresholds for premature ventricular contractions in frog hearts exposed to lithotripter fields (Dalecki), 341

F

Fady, J. F., see Lavandier, B.
Fan, P. H., see Jain, S. P.
Fauser, B. C. J. M., see Pache, T. D.

Femoropopliteal arterial disease
spectral analysis criteria in duplex scanning of aortoiliac and femoropopliteal arterial disease (Legemate), 769

Fetal anomalies
duplex Doppler sonography of the umbilical arteries: predictive value in IUGR and correlation with birth weight (Worrell), 207
prenatal diagnosis, management and outcome of fetal uretero-pelvic junction obstruction (Bosman), 117
sonographic, clinical and genetic aspects of prenatal diagnosis of cystic kidney disease (Reuss), 687

Fetal blood flow
aortic diameter pulse waves and blood flow velocity in the small, for gestational age, fetus (Stale), 471
duplex Doppler sonography of the umbilical arteries: predictive value in IUGR and correlation with birth weight (Worrell), 207
effect of fetal breathing movements on fetal cardiac hemodynamics (van der Mooren), 787
effect of maternal posture on the umbilical artery flow velocity waveform (van Katwijk), 683
flow velocity waveforms in the fetal inferior vena cava during the second half of normal pregnancy (Huisman), 679
waveform pattern recognition—a new semiquantitative method for the analysis of fetal aortic and umbilical artery blood flow velocity recorded by Doppler ultrasound (Malcus), 453

Fetal breathing
effect of fetal breathing movements on fetal cardiac hemodynamics (van der Mooren), 787

Fetal development
duplex Doppler sonography of the umbilical arteries: predictive value in IUGR and correlation with birth weight (Worrell), 207
prenatal diagnosis, management and outcome of fetal uretero-pelvic junction obstruction (Bosman), 117
reversible biochemical changes in the developing rat central nervous system following ultrasound exposure (Margulies), 383

Fetal growth retardation
aortic diameter pulse waves and blood flow velocity in the small, for gestational age, fetus (Stale), 471
duplex Doppler sonography of the umbilical arteries: predictive value in IUGR and correlation with birth weight (Worrell), 207

Fetal renal malformation
prenatal diagnosis, management and outcome of fetal uretero-pelvic junction obstruction (Bosman), 117
sonographic, clinical and genetic aspects of prenatal diagnosis of cystic kidney disease (Reuss), 687

Fetus
aortic diameter pulse waves and blood flow velocity in the small, for gestational age, fetus (Stale), 471
duplex Doppler sonography of the umbilical arteries: predictive value in IUGR and correlation with birth weight (Worrell), 207
effect of fetal breathing movements on fetal cardiac hemodynamics (van der Mooren), 787
flow velocity waveforms in the fetal inferior vena cava during the second half of normal pregnancy (Huisman), 679
in utero measurement of ultrasonically induced fetal mouse temperature increases (Carnes), 373
prenatal diagnosis, management and outcome of fetal uretero-pelvic junction obstruction (Bosman), 117
pulsed ultrasound and neoplastic transformation *in vitro* (Harrison), 627
pulsed ultrasound and the hyperbarically exposed mouse fetus (Child), 367
reversible biochemical changes in the developing rat central nervous system following ultrasound exposure (Margulies), 383
sonographic, clinical and genetic aspects of prenatal diagnosis of cystic kidney disease (Reuss), 687
waveform pattern recognition—a new semiquantitative method for the analysis of fetal aortic and umbilical artery blood flow velocity recorded by Doppler ultrasound (Malcus), 453

FFT
accuracy of velocity and shear rate measurements using pulsed Doppler ultrasound: a comparison of signal analysis techniques (Markou), 803
nonstationarity broadening in pulsed Doppler spectrum measurements (Fish), 147

Fibre orientation
angle-dependent backscatter from the arterial wall (de Kroon), 121

Filipczynski, L. and Wojcik, J.: estimation of transient temperature elevation in lithotripsy and in ultrasonography, 715
Fish, P. J.: nonstationarity broadening in pulsed Doppler spectrum measurements, 147
Fishback, J. L., see Insana, M. F.
Fliescher, A. C., see Worrell, J. A.

Flow
accuracy of velocity and shear rate measurements using pulsed Doppler ultrasound: a comparison of signal analysis techniques (Markou), 803

an investigation of simulated umbilical artery Doppler waveforms. I. The effect of three physical parameters on the maximum frequency envelope and on pulsatility index (Hoskins), 7
an investigation of simulated umbilical artery Doppler waveforms. II. A comparison of three Doppler waveform quality indices (Hoskins), 23
evaluation of Doppler ultrasound for blood perfusion measurements (Eriksson), 445
influence of various instrument settings on the flow information derived from the power mode (Jain), 49
quantitative study of steady flow using color Doppler ultrasound (Tamura), 595

Flow area
influence of various instrument settings on the flow information derived from the power mode (Jain), 49

Flow cytometry
cavitation-generated free radicals during shock wave exposure: investigation with cell-free solutions and suspended cells (Suhr), 761

Flow rig
accuracy of velocity and shear rate measurements using pulsed Doppler ultrasound: a comparison of signal analysis techniques (Markou), 803
an investigation of simulated umbilical artery Doppler waveforms. I. The effect of three physical parameters on the maximum frequency envelope and on pulsatility index (Hoskins), 7
an investigation of simulated umbilical artery Doppler waveforms. II. A comparison of three Doppler waveform quality indices (Hoskins), 23
evaluation of Doppler ultrasound for blood perfusion measurements (Eriksson), 445
influence of various instrument settings on the flow information derived from the power mode (Jain), 49
quantitative study of steady flow using color Doppler ultrasound (Tamura), 595

Fluid properties
a new ultrasonic method for fluid property measurements (Dymling), 497

Fluorescent dyes
cavitation-generated free radicals during shock wave exposure: investigation with cell-free solutions and suspended cells (Suhr), 761

Folberth, W., see Sass, W.
Follett, D. H., see Harris, R. A.

Follicles
transvaginal sonography and abnormal ovarian appearance in menstrual cycle disturbances (Pache), 589

Formalin fixation
influence of histochemical preparation on acoustic parameters of liver tissue: a 5-MHz study (van der Steen), 879

Foster, F. S., see Lockwood, G. R.

Fourier transform
an investigation of simulated umbilical artery Doppler waveforms. II. A comparison of three Doppler waveform quality indices (Hoskins), 23
nonstationarity broadening in pulsed Doppler spectrum measurements (Fish), 147

Fowlkes, J. B., see Rubin, J. M.
Frazier, M. E., see Miller, D. L.
Frazier, M. E., see Miller, D. L.

Free radicals
cavitation-generated free radicals during shock wave exposure: investigation with cell-free solutions and suspended cells (Suhr), 761
sonoluminescence in water and agar gels during irradiation with 0.75 MHz continuous-wave ultrasound (Daniels), 297

Frequency estimation
accuracy of velocity and shear rate measurements using pulsed Doppler ultrasound: a comparison of signal analysis techniques (Markou), 803
adaptive estimation of the mean frequency of a Doppler signal from short data windows (Herment), 901
an investigation of simulated umbilical artery Doppler waveforms. I. The effect of three physical parameters on the maximum frequency envelope and on pulsatility index (Hoskins), 7
an investigation of simulated umbilical artery Doppler waveforms. II. A comparison of three Doppler waveform quality indices (Hoskins), 23
an investigation of simulated umbilical artery Doppler waveforms. III. The effect of noise reduction algorithms on the maximum frequency envelope and on the pulsatility index (Hoskins), 703
computer analysis and pattern recognition of Doppler blood flow spectra for disease classification in the lower limb arteries (Allard), 211
effect of distal occlusions on the assessment of aorto-iliac pathology by analysis of Doppler spectra (Van Asten), 849
nonstationarity broadening in pulsed Doppler spectrum measurements (Fish), 147
spectral composition of Doppler signals (Hoeks), 751
the relative contributions of myocardial wall thickness and ischemia to ultrasonic myocardial integrated backscatter during experimental ischemia (Rijsterborgh), 41
the use of frequency mixing to distinguish size distributions of gas-filled micropores (Quain), 71

Frequency mixing
the use of frequency mixing to distinguish size distributions of gas-filled micropores (Quain), 71

Frequency spectrum
accuracy of velocity and shear rate measurements using pulsed Doppler ultrasound: a comparison of signal analysis techniques (Markou), 803
spectral composition of Doppler signals (Hoeks), 751
the relative contributions of myocardial wall thickness and ischemia to ultrasonic myocardial integrated backscatter during experimental ischemia (Rijsterborgh), 41

Frog
thresholds for premature ventricular contractions in frog hearts exposed to lithotripter fields (Dalecki), 341

Fry, F. J., Reilly, C. R., Dines, D. A., Etchison, M. R. and Trauner, E. J.: absorption in liver at the focus of an ultrasonic shock wave field, 65

G

Gadd, M., see Ritenour, E. R.

Gall bladder
the mechanisms of stone disintegration by shock waves (Sass), 239

Gall stones
the mechanisms of stone disintegration by shock waves (Sass), 239

Gamma rays
synergism between hyperthermia, ultrasound and gamma irradiation (Loverock), 607
ultrasonic cavitation indirectly induces single strand breaks in DNA of viable cells *in vitro* by the action of residual hydrogen peroxide (Miller), 729

Gas bodies
the use of frequency mixing to distinguish size distributions of gas-filled micropores (Quain), 71

Gas bubbles
gauging the likelihood of cavitation from short-pulse, low-duty cycle diagnostic ultrasound (Apfel), 179
mechanisms for hemolysis by ultrasonic cavitation in the rotating exposure system (Miller), 171
the threshold for thermally significant cavitation in dog's thigh muscle *in vivo* (Hynynen), 157
the use of frequency mixing to distinguish size distributions of gas-filled micropores (Quain), 71

Gastric cancer
the ultrasonic properties of gastric cancer tissues obtained with a scanning acoustic microscope system (Saijo), 709

Gates, A. H., see Child, S. Z.

Gaussian beam
pulse-echo imaging using a nondiffracting beam transducer (Lu), 265

Genetic effects
single strand breaks in CHO cell DNA induced by ultrasonic cavitation *in vitro* (Miller), 401

Gennser, G., see Stale, H.
Gimenez, G., see Basset, O.
Gomez, F., see Cathignol, D.
Green, P. S., Ostrem, J. S. and Whitehurst, T. K.: combined reflection and transmission ultrasound imaging, 283
Greenleaf, J. F., see Lu, J.-Y.
Grennberg, A., see Olsson, L.

Groenenberg, I. A. L., Hop, W. C. J. and Wladimiroff, J. W.: Doppler flow velocity waveforms in the fetal cardiac outflow tract: reproducibility of waveform recording and analysis, 583
Guglielmi, J. P., see Herment, A.
Gussenhoven, W. J., see de Kroon, M. G. M.
Gussenhoven, W. J., see de Kroon, M. G. M.

H

Haapanen, A., see Salonen, R.
ter Haar, G. R., see Loverock, P.
Hall, T. J., see Insana, M. F.
Halliwell, M., see Harris, R. A.

Hamster cells
absence of mutagenic effects of continuous and pulsed ultrasound in cultured (A_L) human-hamster hybrid cells (Ritenour), 921

Handa, N., see Maeda, H.

Hard copy device
the use of ink jets in ultrasound registrations (Johansson), 529

Harris, R. A., Follett, D. H., Halliwell, M. and Wells, P. N. T.: ultimate limits in ultrasonic imaging resolution, 547
Harrison, G. H. and Balcer-Kubiczek, E. K.: pulsed ultrasound and neoplastic transformation *in vitro*, 627
Harrison, G. H., see Ritenour, E. R.
Hartman, P. C., Oosterveld, B. J., Thijssen, J. M. and Rosenbusch, G. J. E.: variability of quantitative echographic parameters of the liver: intra- and inter-individual spread, temporal- and age-related effects, 857
He, B. Q., see Yip, Y. P. L.
Heerschap, A., see Smits, G. A. H. J.

Hellmuth Hertz
Carl Hellmuth Hertz (Lindström), 421

Hemodynamics
accuracy of velocity and shear rate measurements using pulsed Doppler ultrasound: a comparison of signal analysis techniques (Markou), 803
effect of distal occlusions on the assessment of aorto-iliac pathology by analysis of Doppler spectra (Van Asten), 849

Hemolysis
mechanisms for hemolysis by ultrasonic cavitation in the rotating exposure system (Miller), 171

Hennerici, M., see Hoeks, A. P. G.

Hepatic veins
change in amplitude distributions of Doppler spectrograms recorded below the aortic valve in patients with a valvular aortic stenosis (Cloutier), 667

Herment, A., Demoment, G., Guglielmi, J. P., Dumee, Ph. and Pellot, C.: adaptive estimation of the mean frequency of a Doppler signal from short data windows, 901
Hertz, C. H., see Dymling, S. O.

Hertz, C. H., see Holmer, N.-G.
Hertz, T. G., see Dymling, S. O.
Hertz, T. G., see Holmer, N.-G.

High-speed films
the mechanisms of stone disintegration by shock waves (Sass), 239

Hilbers, C. W., see Smits, G. A. H. J.
Hill, C. R., Bamber, J. C., Crawford, D. C., Lowe, H. J. and Webb, S.: what might echography learn from imaging science?, 559

Hirsutism
transvaginal sonography and abnormal ovarian appearance in menstrual cycle disturbances (Pache), 589

Histology
early metabolic response to high-energy shock waves in a human tumor kidney xenograft monitored by ^{31}P magnetic resonance spectroscopy (Smits), 791
influence of histochemical preparation on acoustic parameters of liver tissue: a 5-MHz study (van der Steen), 879
measurement of the ultrasonic properties of vascular tissues and blood from 35–65 MHz (Lockwood), 653

Hoeks, A. P. G., Hennerici, M. and Reneman, R. S.: spectral composition of Doppler signals, 751
Hoeneveld, H., see Legemate, D. A.
Hoffman, D., see Child, S. Z.
Holland, C. K., see Apfel, R. E.
Holm, A., Persson, H. W. and Lindström, K.: measurements of ultrasonic fields with optical diffraction tomography, 505
Holm, A., see Holmer, N.-G.
Holmer, N.-G., Almquist, L.-O., Hertz, T. G., Holm, A., Lindstedt, E., Persson, H. W. and Hertz, C. H.: on the mechanism of kidney stone disintegration by acoustic shock waves, 479
Holmer, N.-G., see Johansson, T.
Holmer, N.-G., see Olsson, L.
Holmer, N.-G., see Persson, H. W.
Holmer, N.-G., see Sundström, N.
van Hoorn, W. M., see van der Steen, A. F. W.
Hop, W. C. J., see Groenenberg, I. A. L.
Hop, W. C. J., see Pache, T. D.
Hoskins, P. R.: an investigation of simulated umbilical artery Doppler waveforms. II. A comparison of three Doppler waveform quality indices, 23
Hoskins, P. R.: an investigation of simulated umbilical artery Doppler waveforms. III. The effect of noise reduction algorithms on the maximum frequency envelope and on the pulsatility index, 703
Hoskins, P. R.: clinical trial of umbilical artery Doppler waveform quality indices, 777
Hoskins, P. R., Loupas, T. and McDicken, W. N.: an investigation of simulated umbilical artery Doppler waveforms. I. The effect of three physical parameters on the maximum frequency envelope and on pulsatility index, 7
Hoskins, P. R., Li, S. F. and McDicken, W. N.: velocity estimation using duplex scanners, 195L
Hougaku, H., see Maeda, H.

Huisman, T. W. A., Stewart, P. A. and Wladimiroff, J. W.: flow velocity waveforms in the fetal inferior vena cava during the second half of normal pregnancy, 679
Hülser, D. F., see Suhr, D.

Human lymphocytes
lack of induced increase in sister chromatid exchanges in human lymphocytes exposed to *in vivo* therapeutic ultrasound (Miller), 81

Hunt, J. W., see Lockwood, G. R.

Hydrocephalus
evaluation of cerebral blood flow in rabbits with transcranial Doppler sonography: first results (Tranquart), 815

Hydrogen peroxide
ultrasonic cavitation indirectly induces single strand breaks in DNA of viable cells *in vitro* by the action of residual hydrogen peroxide (Miller), 729

Hydrophones
a measurement system for continuous-wave ultrasound fields (Persson), 501
in situ exposimetry: the ovarian ultrasound examination (Siddiqi), 257
robust electromagnetic probe for the monitoring of lithotriptor output (Pye), 931

Hynynen, W.: the threshold for thermally significant cavitation in dog's thigh muscle *in vivo*, 157

Hyperbaric
pulsed ultrasound and the hyperbarically exposed mouse fetus (Child), 367

Hyperthermia
effect of ultrasound on regional blood flow in neonatal rats (Muscarella), 893
synergism between hyperthermia, ultrasound and gamma irradiation (Loverock), 607
the threshold for thermally significant cavitation in dog's thigh muscle *in vivo* (Hynynen), 157

I

Ilver, J., see Mauritzson, L.

Image processing
an investigation of simulated umbilical artery Doppler waveforms. III. The effect of noise reduction algorithms on the maximum frequency envelope and on the pulsatility index (Hoskins), 703
combined reflection and transmission ultrasound imaging (Green), 283
cyclic changes of blood echogenicity in high-frequency ultrasound (de Kroon), 723
ultimate limits in ultrasonic imaging resolution (Harris), 547
what might echography learn from imaging science? (Hill), 559

Imaging
angle-dependent backscatter from the arterial wall (de Kroon), 121
carotid lesions detected by B-mode ultrasonography in Takayasu's arteritis: "macaroni sign" as an indicator of the disease (Maeda), 695

combined reflection and transmission ultrasound imaging (Green), 283
comparison of four different Doppler instruments used to measure linear and volumetric cardiac output: a study of reproducibility and agreement (Mayo), 347
cyclic changes of blood echogenicity in high-frequency ultrasound (de Kroon), 723
influence of various instrument settings on the flow information derived from the power mode (Jain), 49
measurement of intima-media thickness of common carotid arteries with high-resolution B-mode ultrasonography: inter- and intra-observer variability (Salonen), 225
phase cancellation: a cause of acoustical shadowing at the edges of curved surfaces in B-mode ultrasound images (Rubin), 85
pulse-echo imaging using a nondiffracting beam transducer (Lu), 265
the ultrasonic properties of gastric cancer tissues obtained with a scanning acoustic microscope system (Saijo), 709
ultimate limits in ultrasonic imaging resolution (Harris), 547
ultrasound properties of liver with and without particulate contrast agents (Tuthill), 231
what might echography learn from imaging science? (Hill), 559

Implanted probe
evaluation of cerebral blood flow in rabbits with transcranial Doppler sonography: first results (Tranquart), 815

In ovo *irradiation*
effect of ultrasound on axonal outgrowth in the sympathetic nervous system of the chick (Yip), 139

In situ *exposure*
in situ exposimetry: the ovarian ultrasound examination (Siddiqi), 257
prediction of *in situ* exposure to ultrasound: a proposed standard experimental method (Preston), 333
prediction of *in situ* exposure to ultrasound: an acoustical attenuation method (Preston), 317

In vitro *irradiation*
absence of mutagenic effects of continuous and pulsed ultrasound in cultured (A_L) human-hamster hybrid cells (Ritenour), 921
mechanisms for hemolysis by ultrasonic cavitation in the rotating exposure system (Miller), 171
pulsed ultrasound and neoplastic transformation *in vitro* (Harrison), 627
single strand breaks in CHO cell DNA induced by ultrasonic cavitation *in vitro* (Miller), 401
synergism between hyperthermia, ultrasound and gamma irradiation (Loverock), 607
ultrasonic cavitation indirectly induces single strand breaks in DNA of viable cells *in vitro* by the action of residual hydrogen peroxide (Miller), 729
ultrasound effects on cell proliferation and migration of chick motoneurons (Yip), 55

In vivo *irradiation*
absorption in liver at the focus of an ultrasonic shock wave field (Fry), 65
early metabolic response to high-energy shock waves in a human tumor kid-

ney xenograft monitored by ^{31}P magnetic resonance spectroscopy (Smits), 791
effect of ultrasound on axonal outgrowth in the sympathetic nervous system of the chick (Yip), 139
effects of high-energy shock waves combined with biological response modifiers in different human kidney cancer xenografts (Oosterhof), 391
in situ exposimetry: the ovarian ultrasound examination (Siddiqi), 257
in utero measurement of ultrasonically induced fetal mouse temperature increases (Carnes), 373
lack of induced increase in sister chromatid exchanges in human lymphocytes exposed to *in vivo* therapeutic ultrasound (Miller), 81
pulsed ultrasound and the hyperbarically exposed mouse fetus (Child), 367
reversible biochemical changes in the developing rat central nervous system following ultrasound exposure (Margulies), 383
the threshold for thermally significant cavitation in dog's thigh muscle *in vivo* (Hynynen), 157
thresholds for premature ventricular contractions in frog hearts exposed to lithotripter fields (Dalecki), 341

Inferior vena cava
change in amplitude distributions of Doppler spectrograms recorded below the aortic valve in patients with a valvular aortic stenosis (Cloutier), 667

Ink jet
the use of ink jets in ultrasound registrations (Johansson), 529

Insana, M. F., Hall, T. J. and Fishback, J. L.: identifying acoustic scattering sources in normal renal parenchyma from the anisotropy in acoustic properties, 613

Instrument settings
influence of various instrument settings on the flow information derived from the power mode (Jain), 49

Inter-individual spread
variability of quantitative echographic parameters of the liver: intra- and inter-individual spread, temporal- and age-related effects (Hartman), 857

Inter-observer error
measurement of intima-media thickness of common carotid arteries with high-resolution B-mode ultrasonography: inter- and intra-observer variability (Salonen), 225

Intima-media thickness
carotid lesions detected by B-mode ultrasonography in Takayasu's arteritis: "macaroni sign" as an indicator of the disease (Maeda), 695
measurement of intima-media thickness of common carotid arteries with high-resolution B-mode ultrasonography: inter- and intra-observer variability (Salonen), 225

Intra-arterial imaging
angle-dependent backscatter from the arterial wall (de Kroon), 121

Intra-arterial pressure
effect of distal occlusions on the assessment of aorto-iliac pathology by analysis of Doppler spectra (Van Asten), 849

Intra-individual spread
variability of quantitative echographic parameters of the liver: intra- and inter-individual spread, temporal- and age-related effects (Hartman), 857

Intra-observer error
measurement of intima-media thickness of common carotid arteries with high-resolution B-mode ultrasonography: inter- and intra-observer variability (Salonen), 225

Intra-ocular melanoma
echographic differentiation of histological types of intraocular melanoma (Thijssen), 127

Irradiation
absence of mutagenic effects of continuous and pulsed ultrasound in cultured (A_L) human-hamster hybrid cells (Ritenour), 921
absorption in liver at the focus of an ultrasonic shock wave field (Fry), 65
early metabolic response to high-energy shock waves in a human tumor kidney xenograft monitored by ^{31}P magnetic resonance spectroscopy (Smits), 791
effect of ultrasound on axonal outgrowth in the sympathetic nervous system of the chick (Yip), 139
effect of ultrasound on regional blood flow in neonatal rats (Muscarella), 893
effects of high-energy shock waves combined with biological response modifiers in different human kidney cancer xenografts (Oosterhof), 391
in situ exposimetry: the ovarian ultrasound examination (Siddiqi), 257
in utero measurement of ultrasonically induced fetal mouse temperature increases (Carnes), 373
lack of induced increase in sister chromatid exchanges in human lymphocytes exposed to *in vivo* therapeutic ultrasound (Miller), 81
mechanisms for hemolysis by ultrasonic cavitation in the rotating exposure system (Miller), 171
pulsed ultrasound and neoplastic transformation *in vitro* (Harrison), 627
pulsed ultrasound and the hyperbarically exposed mouse fetus (Child), 367
reversible biochemical changes in the developing rat central nervous system following ultrasound exposure (Margulies), 383
single strand breaks in CHO cell DNA induced by ultrasonic cavitation *in vitro* (Miller), 401
synergism between hyperthermia, ultrasound and gamma irradiation (Loverock), 607
the mechanisms of stone disintegration by shock waves (Sass), 239
the threshold for thermally significant cavitation in dog's thigh muscle *in vivo* (Hynynen), 157
theoretical predictions of the acoustic pressure generated by a shock wave lithotripter (Coleman), 245
thresholds for premature ventricular contractions in frog hearts exposed to lithotripter fields (Dalecki), 341
ultrasonic cavitation indirectly induces single strand breaks in DNA of viable cells *in vitro* by the action of residual hydrogen peroxide (Miller), 729
ultrasound effects on cell proliferation and migration of chick motoneurons (Yip), 55

Ischemia
influence of attenuation on measurements of ultrasonic myocardial integrated backscatter during cardiac cycle (an *in vitro* study) (van der Steen), 869

the relative contributions of myocardial wall thickness and ischemia to ultrasonic myocardial integrated backscatter during experimental ischemia (Rijsterborgh), 41

Itoh, T., see Maeda, H.

J

Jain, S. P., Fan, P. H., Philpot, E. F., Nanda, N. C., Aggarwal, K. K., Moos, S. and Yoganathan, A. P.: influence of various instrument settings on the flow information derived from the power mode, 49

Jarry, M., see Cloutier, G.

Jiang, P., Everbach, E. C. and Apfel, R. E.: applications of mixture laws for predicting the compositions of tissue phantoms, 829

Johansson, T., Nilsson, J., Almquist, L.-O. and Holmer, N.-G.: the use of ink jets in ultrasound registrations, 529

Johnston, K. W., see Tamura, T.

K

Kamada, T., see Maeda, H.

van Katwijk, C. and Wladimiroff, J. W.: effect of maternal posture on the umbilical artery flow velocity waveform, 683

Keller, B. B., see Dalecki, D.

Kelly, R. E., Namon, R. A., Chang, J. Y. and Mantelle, L. L.: evaluation of internal carotid artery stenosis by transcranial Doppler ultrasonography and oculopneumoplethysmography, 577

Kidney

analysis and classification of secondary sounds from the disintegration of kidney stones with acoustic shock waves (Olsson), 491

early metabolic response to high-energy shock waves in a human tumor kidney xenograft monitored by ^{31}P magnetic resonance spectroscopy (Smits), 791

effects of high-energy shock waves combined with biological response modifiers in different human kidney cancer xenografts (Oosterhof), 391

identifying acoustic scattering sources in normal renal parenchyma from the anisotropy in acoustic properties (Insana), 613

on the mechanism of kidney stone disintegration by acoustic shock waves (Holmer), 479

prenatal diagnosis, management and outcome of fetal uretero-pelvic junction obstruction (Bosman), 117

sonographic, clinical and genetic aspects of prenatal diagnosis of cystic kidney disease (Reuss), 687

Kimme-Smith, C., see Tessler, F. N.

Kimura, K., see Maeda, H.

Kremkau, F.: incorrect description of an ultrasonic beam, 411L

de Kroon, M. G. M., van der Wal, L. F., Gussenhoven, W. J. and Bom, N.: angle-dependent backscatter from the arterial wall, 121

de Kroon, M. G. M., Slager, C. J., Gussenhoven, W. J., Serruys, P. W., Roelandt, J. R. T. C. and Bom, N.: cyclic changes of blood echogenicity in high-frequency ultrasound, 723

Ku, D. N., see Markou, C. P.

L

Laminar flow

quantitative study of steady flow using color Doppler ultrasound (Tamura), 595

Lancée, C. T., see Rijsterborgh, H.
Lancée, C. T., see van der Steen, A. F. W.
Langlois, Y. E., see Allard, L.
Langlois, Y. E., see Cloutier, G.

Laser Doppler flowmeter
effect of ultrasound on regional blood flow in neonatal rats (Muscarella), 893

Latour, Y., see Cloutier, G.
Lavandier, B., Muchada, R., Chignier, E., Fady, J. F., Birer, A. and Cathignol, D.: assessment of a potentially noninvasive method for monitoring aortic blood flow in children, 107

Left ventricular outflow tract
change in amplitude distributions of Doppler spectrograms recorded below the aortic valve in patients with a valvular aortic stenosis (Cloutier), 667

Legemate, D. A., Teeuwen, C., Hoeneveld, H., Ackerstaff, R. G. A. and Eikelboom, B. C.: spectral analysis criteria in duplex scanning of aortoiliac and femoropopliteal arterial disease, 769
Lemire, F., see Cloutier, G.
Lenz, P., see Cathignol, D.

Lesion detection
ultrasound properties of liver with and without particulate contrast agents (Tuthill), 231
what might echography learn from imaging science? (Hill), 559

Li, S. F., see Hoskins, P. R.
van Lier, H. J. J., see Van Asten, W. N. J. C.

Light diffraction
measurements of ultrasonic fields with optical diffraction tomography (Holm), 505

Light microscopy
early metabolic response to high-energy shock waves in a human tumor kidney xenograft monitored by ^{31}P magnetic resonance spectroscopy (Smits), 791

Limits, ultimate
ultimate limits in ultrasonic imaging resolution (Harris), 547

Lindstedt, E., see Holmer, N.-G.
Lindström, K.: Carl Hellmuth Hertz, 421
Lindström, K., see Benthin, M.
Lindström, K., see Dymling, S. O.
Lindström, K., see Eriksson, R.
Lindström, K., see Holm, A.
Lindström, K., see Mauritzson, L.
Lindström, K., see Stale, H.

Linear array
two-dimensional airborne ultrasound real-time linear array scanner—applied to screening for scoliosis (Mauritzson), 519

Lithotripsy
analysis and classification of secondary sounds from the disintegration of kidney stones with acoustic shock waves (Olsson), 491
cavitation-generated free radicals during shock wave exposure: investigation with cell-free solutions and suspended cells (Suhr), 761
combined reflection and transmission ultrasound imaging (Green), 283
early metabolic response to high-energy shock waves in a human tumor kidney xenograft monitored by ^{31}P magnetic resonance spectroscopy (Smits), 791
effects of high-energy shock waves combined with biological response modifiers in different human kidney cancer xenografts (Oosterhof), 391
estimation of transient temperature elevation in lithotripsy and in ultrasonography (Filipczynski), 715
influence of water conductivity on the efficacy and the reproducibility of electrohydraulic shock wave generation (Cathignol), 819
on the mechanism of kidney stone disintegration by acoustic shock waves (Holmer), 479
robust electromagnetic probe for the monitoring of lithotriptor output (Pye), 931
the mechanisms of stone disintegration by shock waves (Sass), 239
theoretical predictions of the acoustic pressure generated by a shock wave lithotripter (Coleman), 245
thresholds for premature ventricular contractions in frog hearts exposed to lithotripter fields (Dalecki), 341

Liver
absorption in liver at the focus of an ultrasonic shock wave field (Fry), 65
influence of histochemical preparation on acoustic parameters of liver tissue: a 5-MHz study (van der Steen), 879
ultrasound properties of liver with and without particulate contrast agents (Tuthill), 231
variability of quantitative echographic parameters of the liver: intra- and inter-individual spread, temporal- and age-related effects (Hartman), 857

Lockwood, G. R., Ryan, L. K., Hunt, J. W. and Foster, F. S.: measurement of the ultrasonic properties of vascular tissues and blood from 35–65 MHz, 653
Loupas, T., see Hoskins, P. R.
Loverock, P. and ter Haar, G. R.: synergism between hyperthermia, ultrasound and gamma irradiation, 607
Lowe, H. J., see Hill, C. R.
Lu, J.-Y. and Greenleaf, J. F.: pulse-echo imaging using a nondiffracting beam transducer, 265

Luminal diameter
angle-dependent backscatter from the arterial wall (de Kroon), 121
assessment of a potentially noninvasive method for monitoring aortic blood flow in children (Lavandier), 107

Lymphocytes
lack of induced increase in sister chromatid exchanges in human lymphocytes exposed to *in vivo* therapeutic ultrasound (Miller), 81

M

M-mode imaging
assessment of a potentially noninvasive method for monitoring aortic blood flow in children (Lavandier), 107

Macaroni sign
carotid lesions detected by B-mode ultrasonography in Takayasu's arteritis: "macaroni sign" as an indicator of the disease (Maeda), 695

Madjar, H., Sauerbrei, W., Münch, S. and Schillinger, H.: continuous-wave and pulsed Doppler studies of the breast: clinical results and effect of transducer frequency, 31

Madsen, E. L., see Yao, L. X.

Maeda, H., Handa, N., Matsumoto, M., Hougaku, H., Ogawa, S., Oku, N., Itoh, T., Moriwaki, H., Yoneda, S., Kimura, K. and Kamada, T.: carotid lesions detected by B-mode ultrasonography in Takayasu's arteritis: "macaroni sign" as an indicator of the disease, 695

Magnetic resonance spectroscopy
early metabolic response to high-energy shock waves in a human tumor kidney xenograft monitored by ^{31}P magnetic resonance spectroscopy (Smits), 791

Malcus, P., Andersson, J., Marśal, K. and Olofsson, P. Å.: waveform pattern recognition—a new semiquantitative method for the analysis of fetal aortic and umbilical artery blood flow velocity recorded by Doppler ultrasound, 453

Manco-Johnson, M., see Ritenour, E. R.

Mantelle, L. L., see Kelly, R. E.

Margulies, N., Abraham, V., Way, J. S. and Ziskin, M. C.: reversible biochemical changes in the developing rat central nervous system following ultrasound exposure, 383

Markou, C. P. and Ku, D. N.: accuracy of velocity and shear rate measurements using pulsed Doppler ultrasound: a comparison of signal analysis techniques, 803

Marsál, K., see Malcus, P.

Marsál, K., see Stale, H.

Mastik, F., see Rijsterborgh, H.

Mastik, F., see van der Steen, A. F. W.

Maternal blood pressure
effect of maternal posture on the umbilical artery flow velocity waveform (van Katwijk), 683

Maternal posture
effect of maternal posture on the umbilical artery flow velocity waveform (van Katwijk), 683

Matsumoto, M., see Maeda, H.

Matura, E., see Sass, W.

Maximum frequency envelope
an investigation of simulated umbilical artery Doppler waveforms. III. The effect of noise reduction algorithms on the maximum frequency envelope and on the pulsatility index (Hoskins), 703

Mauritzson, L., Ilver, J., Benoni, G., Lindström, K. and Willner, S.: two-dimensional airborne ultrasound real-time linear array scanner—applied to screening for scoliosis, 519
Mayo, A. and Rawles, J.: comparison of four different Doppler instruments used to measure linear and volumetric cardiac output: a study of reproducibility and agreement, 347
McDicken, W. N., see Hoskins, P. R.
McDicken, W. N., see Hoskins, P. R.
McDicken, W. N., see Pye, S. D.

Mean frequency estimation
adaptive estimation of the mean frequency of a Doppler signal from short data windows (Herment), 901

Mechanical Index
gauging the likelihood of cavitation from short-pulse, low-duty cycle diagnostic ultrasound (Apfel), 179

Melanoma
echographic differentiation of histological types of intraocular melanoma (Thijssen), 127

Membranes
the use of frequency mixing to distinguish size distributions of gas-filled micropores (Quain), 71

Menstrual cycle
transvaginal sonography and abnormal ovarian appearance in menstrual cycle disturbances (Pache), 589

Mestas, J. L., see Basset, O.
Mestas, J. L., see Cathignol, D.
Meyer, R. A., see Siddiqi, T. A.

Mice
in utero measurement of ultrasonically induced fetal mouse temperature increases (Carnes), 373
pulsed ultrasound and neoplastic transformation *in vitro* (Harrison), 627
pulsed ultrasound and the hyperbarically exposed mouse fetus (Child), 367

Micropores
the use of frequency mixing to distinguish size distributions of gas-filled micropores (Quain), 71

Microscope
angle-dependent backscatter from the arterial wall (de Kroon), 121
the ultrasonic properties of gastric cancer tissues obtained with a scanning acoustic microscope system (Saijo), 709

Middle cerebral artery
evaluation of internal carotid artery stenosis by transcranial Doppler ultrasonography and oculopneumoplethysmography (Kelly), 577

Miller, D. L., Thomas, R. M. and Frazier, M. E.: single strand breaks in CHO cell DNA induced by ultrasonic cavitation *in vitro*, 401

Miller, D. L., Thomas, R. M. and Frazier, M. E.: ultrasonic cavitation indirectly induces single strand breaks in DNA of viable cells *in vitro* by the action of residual hydrogen peroxide, 729
Miller, D. L., Thomas, R. M. and Williams, A. R.: mechanisms for hemolysis by ultrasonic cavitation in the rotating exposure system, 171
Miller, M. W., Azadniv, M., Cox, C. and Miller, W. M.: lack of induced increase in sister chromatid exchanges in human lymphocytes exposed to *in vivo* therapeutic ultrasound, 81
Miller, M. W., see Quain, R. M.
Miller, W. M., see Miller, M. W.
Miodovnik, M., see Siddiqi, T. A.

Mixture laws
applications of mixture laws for predicting the compositions of tissue phantoms (Jiang), 829

Model
accuracy of velocity and shear rate measurements using pulsed Doppler ultrasound: a comparison of signal analysis techniques (Markou), 803
an investigation of simulated umbilical artery Doppler waveforms. I. The effect of three physical parameters on the maximum frequency envelope and on pulsatility index (Hoskins), 7
an investigation of simulated umbilical artery Doppler waveforms. II. A comparison of three Doppler waveform quality indices (Hoskins), 23
applications of mixture laws for predicting the compositions of tissue phantoms (Jiang), 829
assessment of a potentially noninvasive method for monitoring aortic blood flow in children (Lavandier), 107
estimation of transient temperature elevation in lithotripsy and in ultrasonography (Filipczynski), 715
evaluation of Doppler ultrasound for blood perfusion measurements (Eriksson), 445
identifying acoustic scattering sources in normal renal parenchyma from the anisotropy in acoustic properties (Insana), 613
in utero measurement of ultrasonically induced fetal mouse temperature increases (Carnes), 373
influence of various instrument settings on the flow information derived from the power mode (Jain), 49
measurement of blood perfusion in tissue using Doppler ultrasound (Dymling), 433
nonstationarity broadening in pulsed Doppler spectrum measurements (Fish), 147
phase cancellation: a cause of acoustical shadowing at the edges of curved surfaces in B-mode ultrasound images (Rubin), 85
statistical uncertainty in ultrasonic backscatter and attenuation coefficients determined with a reference phantom (Yao), 187
theoretical predictions of the acoustic pressure generated by a shock wave lithotripter (Coleman), 245

Modulated ink jet
the use of ink jets in ultrasound registrations (Johansson), 529

van der Mooren, K., Wladimiroff, J. W. and Stijnen, T.: effect of fetal breathing movements on fetal cardiac hemodynamics, 787

Moos, S., see Jain, S. P.
Moriwaki, H., see Maeda, H.

Morphology
echographic differentiation of histological types of intraocular melanoma (Thijssen), 127

Motion
evaluation of Doppler ultrasound for blood perfusion measurements (Eriksson), 445
measurement of blood perfusion in tissue using Doppler ultrasound (Dymling), 433
the relative contributions of myocardial wall thickness and ischemia to ultrasonic myocardial integrated backscatter during experimental ischemia (Rijsterborgh), 41

Motion artifacts
evaluation of Doppler ultrasound for blood perfusion measurements (Eriksson), 445
measurement of blood perfusion in tissue using Doppler ultrasound (Dymling), 433

Motoneuron
ultrasound effects on cell proliferation and migration of chick motoneurons (Yip), 55

Mouse
in utero measurement of ultrasonically induced fetal mouse temperature increases (Carnes), 373
pulsed ultrasound and neoplastic transformation *in vitro* (Harrison), 627
pulsed ultrasound and the hyperbarically exposed mouse fetus (Child), 367

Muchada, R., see Lavandier, B.
Münch, S., see Madjar, H.
Munro, E. G., see Pye, S. D.
Muscarella, L. F., Vasthare, U., Tuma, R. F., Abraham, V. and Ziskin, M. C.: effect of ultrasound on regional blood flow in neonatal rats, 893

Mutation
absence of mutagenic effects of continuous and pulsed ultrasound in cultured (A_L) human-hamster hybrid cells (Ritenour), 921

Myocardium
influence of attenuation on measurements of ultrasonic myocardial integrated backscatter during cardiac cycle (an *in vitro* study) (van der Steen), 869
the relative contributions of myocardial wall thickness and ischemia to ultrasonic myocardial integrated backscatter during experimental ischemia (Rijsterborgh), 41

N

Namon, R. A., see Kelly, R. E.
Nanda, N. C., see Jain, S. P.
Neel, D. S., see Dalecki, D.

Neoplastic transformation
pulsed ultrasound and neoplastic transformation *in vitro* (Harrison), 627

Neovascularisation
continuous-wave and pulsed Doppler studies of the breast: clinical results and effect of transducer frequency (Madjar), 31

Neural development
effect of ultrasound on axonal outgrowth in the sympathetic nervous system of the chick (Yip), 139
ultrasound effects on cell proliferation and migration of chick motoneurons (Yip), 55

Niermeyer, M. F., see Reuss, A.
Nijman, J. M., see Bosman, G.
Nilsson, J., see Johansson, T.

Noise
an investigation of simulated umbilical artery Doppler waveforms. I. The effect of three physical parameters on the maximum frequency envelope and on pulsatility index (Hoskins), 7
an investigation of simulated umbilical artery Doppler waveforms. II. A comparison of three Doppler waveform quality indices (Hoskins), 23
an investigation of simulated umbilical artery Doppler waveforms. III. The effect of noise reduction algorithms on the maximum frequency envelope and on the pulsatility index (Hoskins), 703

Nondiffracting beam
pulse-echo imaging using a nondiffracting beam transducer (Lu), 265

Nondiffracting transducer
pulse-echo imaging using a nondiffracting beam transducer (Lu), 265

Nonlinear acoustic phenomena
absorption in liver at the focus of an ultrasonic shock wave field (Fry), 65
the use of frequency mixing to distinguish size distributions of gas-filled micropores (Quain), 71

Nonlinear parameter
applications of mixture laws for predicting the compositions of tissue phantoms (Jiang), 829

Nonstationarity
nonstationarity broadening in pulsed Doppler spectrum measurements (Fish), 147

Noordergraaf, A., see Dalecki, D.
Norbash, S. G., see Yip, Y. P.
Norton, S., see Child, S. Z.

NU-1 kidney tumor xenograft
early metabolic response to high-energy shock waves in a human tumor kidney xenograft monitored by ^{31}P magnetic resonance spectroscopy (Smits), 791

O

O'Brien, Jr., W. D., see Siddiqi, T. A.

Observer variability
measurement of intima-media thickness of common carotid arteries with high-resolution B-mode ultrasonography: inter- and intra-observer variability (Salonen), 225

Obstetrics
an investigation of simulated umbilical artery Doppler waveforms. I. The effect of three physical parameters on the maximum frequency envelope and on pulsatility index (Hoskins), 7
duplex Doppler sonography of the umbilical arteries: predictive value in IUGR and correlation with birth weight (Worrell), 207
effect of maternal posture on the umbilical artery flow velocity waveform (van Katwijk), 683
estimation of transient temperature elevation in lithotripsy and in ultrasonography (Filipczynski), 715
flow velocity waveforms in the fetal inferior vena cava during the second half of normal pregnancy (Huisman), 679
prenatal diagnosis, management and outcome of fetal uretero-pelvic junction obstruction (Bosman), 117
sonographic, clinical and genetic aspects of prenatal diagnosis of cystic kidney disease (Reuss), 687
waveform pattern recognition—a new semiquantitative method for the analysis of fetal aortic and umbilical artery blood flow velocity recorded by Doppler ultrasound (Malcus), 453

Oculopneumoplethysmography
evaluation of internal carotid artery stenosis by transcranial Doppler ultrasonography and oculopneumoplethysmography (Kelly), 577

Ogawa, S., see Maeda, H.
Okawai, H., see Saijo, Y.
Oku, N., see Maeda, H.

Oligomenorrhea
transvaginal sonography and abnormal ovarian appearance in menstrual cycle disturbances (Pache), 589

Olofsson, P. Å., see Malcus, P.
Olsson, L., Almquist, L.-O., Grennberg, A. and Holmer, N.-G.: analysis and classification of secondary sounds from the disintegration of kidney stones with acoustic shock waves, 491
Olsson, L., see Sundström, N.
Oosterhof, G. O. N., Smits, G. A. H. J., de Ruyter, A. E., Schalken, J. A. and Debruyne, F. M. J.: effects of high-energy shock waves combined with biological response modifiers in different human kidney cancer xenografts, 391
Oosterhof, G. O. N., see Smits, G. A. H. J.
Oosterhuis, J. A., see Thijssen, J. M.
Oosterveld, B. J., see Hartman, P. C.
Ophir, J., see Robinson, D. E.

Optical diffraction
measurements of ultrasonic fields with optical diffraction tomography (Holm), 505

Ostrem, J. S., see Green, P. S.

Ovary
transvaginal sonography and abnormal ovarian appearance in menstrual cycle disturbances (Pache), 589

P

^{31}P magnetic resonance spectroscopy
early metabolic response to high-energy shock waves in a human tumor kidney xenograft monitored by ^{31}P magnetic resonance spectroscopy (Smits), 791

Pache, T. D., Hop, W. C. J., Wladimiroff, J. W., Schipper, J. and Fauser, B. C. J. M.: transvaginal sonography and abnormal ovarian appearance in menstrual cycle disturbances, 589
Palladino, J. L., see Dalecki, D.

Paraffin embedding
influence of histochemical preparation on acoustic parameters of liver tissue: a 5-MHz study (van der Steen), 879

Parker, K. J., see Tuthill, P. A.
Parker, R., see Ritenour, E. R.
Parr, N. J., see Pye, S. D.

Pattern recognition
computer analysis and pattern recognition of Doppler blood flow spectra for disease classification in the lower limb arteries (Allard), 211
waveform pattern recognition—a new semiquantitative method for the analysis of fetal aortic and umbilical artery blood flow velocity recorded by Doppler ultrasound (Malcus), 453
what might echography learn from imaging science? (Hill), 559

Pellot, C., see Herment, A.

Perception
what might echography learn from imaging science? (Hill), 559

Perfusion
evaluation of Doppler ultrasound for blood perfusion measurements (Eriksson), 445
measurement of blood perfusion in tissue using Doppler ultrasound (Dymling), 433

Persson, H. W., Dymling, S. O. and Holmer, N.-G.: a measurement system for continuous-wave ultrasound fields, 501
Persson, H. W., see Dymling, S. O.
Persson, H. W., see Dymling, S. O.
Persson, H. W., see Eriksson, R.
Persson, H. W., see Holm, A.
Persson, H. W., see Holmer, N.-G.
Persson, H. W., see Sundström, N.

Phantom
accuracy of velocity and shear rate measurements using pulsed Doppler ultrasound: a comparison of signal analysis techniques (Markou), 803
an investigation of simulated umbilical artery Doppler waveforms. I. The effect of three physical parameters on the maximum frequency envelope and on pulsatility index (Hoskins), 7
an investigation of simulated umbilical artery Doppler waveforms. II. A comparison of three Doppler waveform quality indices (Hoskins), 23
applications of mixture laws for predicting the compositions of tissue phantoms (Jiang), 829
author's reply to "velocity estimation using duplex scanners," 195L (Tessler), 199L
evaluation of Doppler ultrasound for blood perfusion measurements (Eriksson), 445
phase cancellation: a cause of acoustical shadowing at the edges of curved surfaces in B-mode ultrasound images (Rubin), 85
pulse-echo imaging using a nondiffracting beam transducer (Lu), 265
statistical uncertainty in ultrasonic backscatter and attenuation coefficients determined with a reference phantom (Yao), 187
velocity estimation using duplex scanners (Hoskins), 195L
volume measurement by ultrasonic transverse or sagittal cross-sectional scanning (Basset), 291

Phase aberration
ultimate limits in ultrasonic imaging resolution (Harris), 547

Phase cancellation
phase cancellation: a cause of acoustical shadowing at the edges of curved surfaces in B-mode ultrasound images (Rubin), 85

Philpot, E. F., see Jain, S. P.

Pig
the relative contributions of myocardial wall thickness and ischemia to ultrasonic myocardial integrated backscatter during experimental ischemia (Rijsterborgh), 41

Placental sluice flow
effect of maternal posture on the umbilical artery flow velocity waveform (van Katwijk), 683

Plaque
angle-dependent backscatter from the arterial wall (de Kroon), 121

Plethysmography, ocular
evaluation of internal carotid artery stenosis by transcranial Doppler ultrasonography and oculopneumoplethysmography (Kelly), 577

Poiseuille flow
quantitative study of steady flow using color Doppler ultrasound (Tamura), 595

Polycystic ovary
transvaginal sonography and abnormal ovarian appearance in menstrual cycle disturbances (Pache), 589

Pores
the use of frequency mixing to distinguish size distributions of gas-filled micropores (Quain), 71

Porous membranes
the use of frequency mixing to distinguish size distributions of gas-filled micropores (Quain), 71

Posture
effect of maternal posture on the umbilical artery flow velocity waveform (van Katwijk), 683

Pourcelot, L., see Tranquart, F.

Premature ventricular contraction
thresholds for premature ventricular contractions in frog hearts exposed to lithotripter fields (Dalecki), 341

Preparation, histologic
influence of histochemical preparation on acoustic parameters of liver tissue: a 5-MHz study (van der Steen), 879

Pressure
absence of mutagenic effects of continuous and pulsed ultrasound in cultured (A_L) human-hamster hybrid cells (Ritenour), 921
in situ exposimetry: the ovarian ultrasound examination (Siddiqi), 257
influence of water conductivity on the efficacy and the reproducibility of electrohydraulic shock wave generation (Cathignol), 819
pulsed ultrasound and neoplastic transformation *in vitro* (Harrison), 627
pulsed ultrasound and the hyperbarically exposed mouse fetus (Child), 367
the mechanisms of stone disintegration by shock waves (Sass), 239
theoretical predictions of the acoustic pressure generated by a shock wave lithotripter (Coleman), 245

Preston, R. C., Shaw, W. and Zeqiri, B.: prediction of *in situ* exposure to ultrasound: a proposed standard experimental method, 333
Preston, R. C., Shaw, W. and Zeqiri, B.: prediction of *in situ* exposure to ultrasound: an acoustical attenuation method, 317
Price, D. J., see Daniels, S.
Priesmeyer, H.-G., see Sass, W.

Printer
the use of ink jets in ultrasound registrations (Johansson), 529

Prostate
volume measurement by ultrasonic transverse or sagittal cross-sectional scanning (Basset), 291

Psycophysics
what might echography learn from imaging science? (Hill), 559

Pulsatility index
an investigation of simulated umbilical artery Doppler waveforms. I. The effect of three physical parameters on the maximum frequency envelope and on pulsatility index (Hoskins), 7

an investigation of simulated umbilical artery Doppler waveforms. II. A comparison of three Doppler waveform quality indices (Hoskins), 23
an investigation of simulated umbilical artery Doppler waveforms. III. The effect of noise reduction algorithms on the maximum frequency envelope and on the pulsatility index (Hoskins), 703
clinical trial of umbilical artery Doppler waveform quality indices (Hoskins), 777
effect of maternal posture on the umbilical artery flow velocity waveform (van Katwijk), 683
evaluation of internal carotid artery stenosis by transcranial Doppler ultrasonography and oculopneumoplethysmography (Kelly), 577

Pulse wave velocity
calculation of pulse-wave velocity using cross correlation—effects of reflexes in the arterial tree (Benthin), 461

Pulsed Doppler
accuracy of velocity and shear rate measurements using pulsed Doppler ultrasound: a comparison of signal analysis techniques (Markou), 803
assessment of a potentially noninvasive method for monitoring aortic blood flow in children (Lavandier), 107
comparison of four different Doppler instruments used to measure linear and volumetric cardiac output: a study of reproducibility and agreement (Mayo), 347
continuous-wave and pulsed Doppler studies of the breast: clinical results and effect of transducer frequency (Madjar), 31
evaluation of internal carotid artery stenosis by transcranial Doppler ultrasonography and oculopneumoplethysmography (Kelly), 577
influence of various instrument settings on the flow information derived from the power mode (Jain), 49
nonstationarity broadening in pulsed Doppler spectrum measurements (Fish), 147
spectral analysis criteria in duplex scanning of aortoiliac and femoropopliteal arterial disease (Legemate), 769

Pye, S. D., Parr, N. J., Munro, E. G., Anderson, T. and McDicken, W. N.: robust electromagnetic probe for the monitoring of lithotriptor output, 931

Q

Quain, R. M., Waag, R. C. and Miller, M. W.: the use of frequency mixing to distinguish size distributions of gas-filled micropores, 71

Quantitative parameters
variability of quantitative echographic parameters of the liver: intra- and interindividual spread, temporal- and age-related effects (Hartman), 857

R

Rabbit
evaluation of cerebral blood flow in rabbits with transcranial Doppler sonography: first results (Tranquart), 815

Radiation force
a new ultrasonic method for fluid property measurements (Dymling), 497

Rat
absorption in liver at the focus of an ultrasonic shock wave field (Fry), 65
effect of ultrasound on regional blood flow in neonatal rats (Muscarella), 893
reversible biochemical changes in the developing rat central nervous system following ultrasound exposure (Margulies), 383

Rawles, J., see Mayo, A.

Ray tracing
phase cancellation: a cause of acoustical shadowing at the edges of curved surfaces in B-mode ultrasound images (Rubin), 85
regions in the B-mode image of a cylinder where the location of a point reflector is changed by sound speed variation (Soetanto), 355

Reference values
statistical uncertainty in ultrasonic backscatter and attenuation coefficients determined with a reference phantom (Yao), 187

Reflection
combined reflection and transmission ultrasound imaging (Green), 283
phase cancellation: a cause of acoustical shadowing at the edges of curved surfaces in B-mode ultrasound images (Rubin), 85

Refraction
phase cancellation: a cause of acoustical shadowing at the edges of curved surfaces in B-mode ultrasound images (Rubin), 85
regions in the B-mode image of a cylinder where the location of a point reflector is changed by sound speed variation (Soetanto), 355

Reid, J. M., see Soetanto, K.
Reilly, C. R., see Fry, F. J.

Renal tissue
identifying acoustic scattering sources in normal renal parenchyma from the anisotropy in acoustic properties (Insana), 613

Reneman, R. S., see Hoeks, A. P. G.

Reports, meetings
1990 IEEE Ultrasonics Symposia (Shung, Daft and O'Donnell), 407

Reproducibility
assessment of a potentially noninvasive method for monitoring aortic blood flow in children (Lavandier), 107
comparison of four different Doppler instruments used to measure linear and volumetric cardiac output: a study of reproducibility and agreement (Mayo), 347

Resistance index
duplex Doppler sonography of the umbilical arteries: predictive value in IUGR and correlation with birth weight (Worrell), 207
evaluation of cerebral blood flow in rabbits with transcranial Doppler sonography: first results (Tranquart), 815

Resolution
ultimate limits in ultrasonic imaging resolution (Harris), 547

Resonant bubbles
the use of frequency mixing to distinguish size distributions of gas-filled micropores (Quain), 71

Reuss, A., Wladimiroff, J. W. and Niermeyer, M. F.: sonographic, clinical and genetic aspects of prenatal diagnosis of cystic kidney disease, 687
Reuss, A., see Bosman, G.

Reviews, book
Bioeffects: Williams (Kremkau), 737
Diagnostic ultrasound and animal reproduction: Taverne and Willemse (van Camp), 738
Doppler ultrasound: principles and instruments: Kremkau (Wells), 739
Duplex scanning in vascular disorders: Strandness (Thiele), 737
Gastrointestinal ultrasonography clinics in diagnostic ultrasound 23: Kurtz and Goldberg (Lyons and Ke), 841
Noninvasive techniques in biology and medicine: Freeman, Fukushima and Greene (Evans), 840
Physics and instrumentation of diagnostic medical ultrasound: Fish (Gill), 738
Practical color atlas of sectional anatomy: Lyons (Greenbaum), 839
Practical echocardiography and Doppler: Monaghan (Usher), 309
Ultrasound in coronary artery disease: present role and future perspective: Iliceto, Rizzon, and Roelandt (Shah), 840
Video atlas of two-dimensional color flow Doppler echocardiography: Gura (Nanna), 839

R.F. analysis
angle-dependent backscatter from the arterial wall (de Kroon), 121
echographic differentiation of histological types of intraocular melanoma (Thijssen), 127
ultimate limits in ultrasonic imaging resolution (Harris), 547

Rijsterborgh, H., Mastik, F., Lancée, C. T., Sassen, L. M. A., Verdouw, P. D., Roelandt, J. and Bom, N.: the relative contributions of myocardial wall thickness and ischemia to ultrasonic myocardial integrated backscatter during experimental ischemia, 41
Rijsterborgh, H., see van der Steen, A. F. W.
Ritenour, E. R., Braaton, M., Harrison, G. H., Ueno, A., Gadd, M., Manco-Johnson, M., Parker, R., Shih, S. and Waldren, C. A.: absence of mutagenic effects of continuous and pulsed ultrasound in cultured (A_L) human-hamster hybrid cells, 921
Robillard, P., see Allard, L.
Robinson, D. E., Ophir, J., Wilson, L. S. and Chen, C. F.: pulse-echo ultrasound speed measurements: progress and prospects, 633
Roederer, G. O., see Allard, L.
Roelandt, J. R. T. C., see de Kroon, M. G. M.
Roelandt, J., see Rijsterborgh, H.
Romijn, R. L., see Thijssen, J. M.
Roncin, A., see Tranquart, F.
Rosenbusch, G. J. E., see Hartman, P. C.
Rosenthal, M. S., see Yip, Y. P.
Rosenthal, M. S., see Yip, Y. P. L.
Roy, P., see Allard, L.
Rubin, J. M., Adler, R. S., Fowlkes, J. B. and Carson, P. L.: phase cancellation: a cause of acoustical shadowing at the edges of curved surfaces in B-mode ultrasound images, 85

Ruys, J. H. J., see Smits, G. A. H. J.
de Ruyter, A. E., see Oosterhof, G. O. N.
Ruzicka, R., see Benthin, M.
Ryan, L. K., see Lockwood, G. R.

S

Safety
absence of mutagenic effects of continuous and pulsed ultrasound in cultured (A_L) human-hamster hybrid cells (Ritenour), 921
estimation of transient temperature elevation in lithotripsy and in ultrasonography (Filipczynski), 715
in situ exposimetry: the ovarian ultrasound examination (Siddiqi), 257
in utero measurement of ultrasonically induced fetal mouse temperature increases (Carnes), 373
prediction of *in situ* exposure to ultrasound: a proposed standard experimental method (Preston), 333
prediction of *in situ* exposure to ultrasound: an acoustical attenuation method (Preston), 317
pulsed ultrasound and the hyperbarically exposed mouse fetus (Child), 367
reversible biochemical changes in the developing rat central nervous system following ultrasound exposure (Margulies), 383
thresholds for premature ventricular contractions in frog hearts exposed to lithotripter fields (Dalecki), 341

Saijo, Y., Tanaka, M., Okawai, H. and Dunn, F.: the ultrasonic properties of gastric cancer tissues obtained with a scanning acoustic microscope system, 709
Salonen, J. T., see Salonen, R.
Salonen, R., Haapanen, A. and Salonen, J. T.: measurement of intima-media thickness of common carotid arteries with high-resolution B-mode ultrasonography: inter- and intra-observer variability, 225

SAM
the ultrasonic properties of gastric cancer tissues obtained with a scanning acoustic microscope system (Saijo), 709

Sass, W., Bräunlich, M., Dreyer, H.-P., Matura, E., Folberth, W., Priesmeyer, H.-G. and Seifert, J.: the mechanisms of stone disintegration by shock waves, 239
Sassen, L. M. A., see Rijsterborgh, H.
Sauerbrei, W., see Madjar, H.
Saunders, F. W., see White, D. N.
Saunders, J. E., see Coleman, A. J.

Scan format
phase cancellation: a cause of acoustical shadowing at the edges of curved surfaces in B-mode ultrasound images (Rubin), 85

Scanner
two-dimensional airborne ultrasound real-time linear array scanner—applied to screening for scoliosis (Mauritzson), 519

Scanning acoustic microscope
the ultrasonic properties of gastric cancer tissues obtained with a scanning acoustic microscope system (Saijo), 709

Scattering
combined reflection and transmission ultrasound imaging (Green), 283
cyclic changes of blood echogenicity in high-frequency ultrasound (de Kroon), 723
identifying acoustic scattering sources in normal renal parenchyma from the anisotropy in acoustic properties (Insana), 613
measurement of the ultrasonic properties of vascular tissues and blood from 35–65 MHz (Lockwood), 653
the relative contributions of myocardial wall thickness and ischemia to ultrasonic myocardial integrated backscatter during experimental ischemia (Rijsterborgh), 41
ultrasound properties of liver with and without particulate contrast agents (Tuthill), 231

Scavengers
cavitation-generated free radicals during shock wave exposure: investigation with cell-free solutions and suspended cells (Suhr), 761

Schalken, J. A., see Oosterhof, G. O. N.
Schalken, J. A., see Smits, G. A. H. J.
Schillinger, H., see Madjar, H.
Schipper, J., see Pache, T. D.

Scoliosis
two-dimensional airborne ultrasound real-time linear array scanner—applied to screening for scoliosis (Mauritzson), 519

Secondary sounds
analysis and classification of secondary sounds from the disintegration of kidney stones with acoustic shock waves (Olsson), 491
on the mechanism of kidney stone disintegration by acoustic shock waves (Holmer), 479

Seifert, J., see Sass, W.
Serruys, P. W., see de Kroon, M. G. M.

Shadows
phase cancellation: a cause of acoustical shadowing at the edges of curved surfaces in B-mode ultrasound images (Rubin), 85

Shah, D. M., see Worrell, J. A.
Shaw, W., see Preston, R. C.
Shaw, W., see Preston, R. C.

Shear rate
accuracy of velocity and shear rate measurements using pulsed Doppler ultrasound: a comparison of signal analysis techniques (Markou), 803

Shih, S., see Ritenour, E. R.

Shock waves
absorption in liver at the focus of an ultrasonic shock wave field (Fry), 65
analysis and classification of secondary sounds from the disintegration of kidney stones with acoustic shock waves (Olsson), 491
cavitation-generated free radicals during shock wave exposure: investigation with cell-free solutions and suspended cells (Suhr), 761

estimation of transient temperature elevation in lithotripsy and in ultrasonography (Filipczynski), 715
influence of water conductivity on the efficacy and the reproducibility of electrohydraulic shock wave generation (Cathignol), 819
on the mechanism of kidney stone disintegration by acoustic shock waves (Holmer), 479
robust electromagnetic probe for the monitoring of lithotriptor output (Pye), 931
the mechanisms of stone disintegration by shock waves (Sass), 239
theoretical predictions of the acoustic pressure generated by a shock wave lithotripter (Coleman), 245

Siddiqi, T. A., O'Brien, Jr., W. D., Meyer, R. A., Sullivan, J. M. and Miodovnik, M.: *in situ* exposimetry: the ovarian ultrasound examination, 257

Sidelobes
pulse-echo imaging using a nondiffracting beam transducer (Lu), 265

Signal averaging
ultimate limits in ultrasonic imaging resolution (Harris), 547

Signal processing
accuracy of velocity and shear rate measurements using pulsed Doppler ultrasound: a comparison of signal analysis techniques (Markou), 803
angle-dependent backscatter from the arterial wall (de Kroon), 121
nonstationarity broadening in pulsed Doppler spectrum measurements (Fish), 147
spectral composition of Doppler signals (Hoeks), 751
ultimate limits in ultrasonic imaging resolution (Harris), 547

Sister chromatid exchange
lack of induced increase in sister chromatid exchanges in human lymphocytes exposed to *in vivo* therapeutic ultrasound (Miller), 81

Skin contours
registration of surface structures using airborne focused ultrasound (Sundström), 513

Skotnicki, S. H., see Van Asten, W. N. J. C.
Slager, C. J., see de Kroon, M. G. M.
Smits, G. A. H. J., Heerschap, A., Oosterhof, G. O. N., Ruys, J. H. J., Hilbers, C. W., Debruyne, F. M. J. and Schalken, J. A.: early metabolic response to high-energy shock waves in a human tumor kidney xenograft monitored by ^{31}P magnetic resonance spectroscopy, 791
Smits, G. A. H. J., see Oosterhof, G. O. N.
Soetanto, K. and Reid, J. M.: regions in the B-mode image of a cylinder where the location of a point reflector is changed by sound speed variation, 355
Solignac, A., see Cloutier, G.

Sonoluminescence
sonoluminescence in water and agar gels during irradiation with 0.75 MHz continuous-wave ultrasound (Daniels), 297

Spatial resolution
ultimate limits in ultrasonic imaging resolution (Harris), 547

Speckle
an investigation of simulated umbilical artery Doppler waveforms. I. The effect of three physical parameters on the maximum frequency envelope and on pulsatility index (Hoskins), 7
an investigation of simulated umbilical artery Doppler waveforms. III. The effect of noise reduction algorithms on the maximum frequency envelope and on the pulsatility index (Hoskins), 703
ultrasound properties of liver with and without particulate contrast agents (Tuthill), 231
what might echography learn from imaging science? (Hill), 559

Spectral analysis
accuracy of velocity and shear rate measurements using pulsed Doppler ultrasound: a comparison of signal analysis techniques (Markou), 803
an investigation of simulated umbilical artery Doppler waveforms. I. The effect of three physical parameters on the maximum frequency envelope and on pulsatility index (Hoskins), 7
an investigation of simulated umbilical artery Doppler waveforms. II. A comparison of three Doppler waveform quality indices (Hoskins), 23
analysis and classification of secondary sounds from the disintegration of kidney stones with acoustic shock waves (Olsson), 491
change in amplitude distributions of Doppler spectrograms recorded below the aortic valve in patients with a valvular aortic stenosis (Cloutier), 667
clinical trial of umbilical artery Doppler waveform quality indices (Hoskins), 777
continuous-wave and pulsed Doppler studies of the breast: clinical results and effect of transducer frequency (Madjar), 31
effect of distal occlusions on the assessment of aorto-iliac pathology by analysis of Doppler spectra (Van Asten), 849
measurement of blood perfusion in tissue using Doppler ultrasound (Dymling), 433
nonstationarity broadening in pulsed Doppler spectrum measurements (Fish), 147
spectral analysis criteria in duplex scanning of aortoiliac and femoropopliteal arterial disease (Legemate), 769
spectral composition of Doppler signals (Hoeks), 751

Spectral broadening
an investigation of simulated umbilical artery Doppler waveforms. I. The effect of three physical parameters on the maximum frequency envelope and on pulsatility index (Hoskins), 7
an investigation of simulated umbilical artery Doppler waveforms. II. A comparison of three Doppler waveform quality indices (Hoskins), 23
author's reply to "velocity estimation using duplex scanners," 195L (Tessler), 199L
effect of distal occlusions on the assessment of aorto-iliac pathology by analysis of Doppler spectra (Van Asten), 849
nonstationarity broadening in pulsed Doppler spectrum measurements (Fish), 147
quantitative study of steady flow using color Doppler ultrasound (Tamura), 595
spectral composition of Doppler signals (Hoeks), 751
velocity estimation using duplex scanners (Hoskins), 195L

Speed of sound
applications of mixture laws for predicting the compositions of tissue phantoms (Jiang), 829
identifying acoustic scattering sources in normal renal parenchyma from the anisotropy in acoustic properties (Insana), 613
influence of histochemical preparation on acoustic parameters of liver tissue: a 5-MHz study (van der Steen), 879
measurement of the ultrasonic properties of vascular tissues and blood from 35–65 MHz (Lockwood), 653
phase cancellation: a cause of acoustical shadowing at the edges of curved surfaces in B-mode ultrasound images (Rubin), 85
pulse-echo ultrasound speed measurements: progress and prospects (Robinson), 633
regions in the B-mode image of a cylinder where the location of a point reflector is changed by sound speed variation (Soetanto), 355
the ultrasonic properties of gastric cancer tissues obtained with a scanning acoustic microscope system (Saijo), 709
ultrasound properties of liver with and without particulate contrast agents (Tuthill), 231

Stale, H., Marsál, K., Gennser, G., Benthin, M., Dahl, P. and Lindström, K.: aortic diameter pulse waves and blood flow velocity in the small, for gestational age, fetus, 471

Standards
prediction of *in situ* exposure to ultrasound: a proposed standard experimental method (Preston), 333
prediction of *in situ* exposure to ultrasound: an acoustical attenuation method (Preston), 317

Stationarity
nonstationarity broadening in pulsed Doppler spectrum measurements (Fish), 147

Statistical uncertainty
statistical uncertainty in ultrasonic backscatter and attenuation coefficients determined with a reference phantom (Yao), 187

van der Steen, A. F. W., Cuypers, M. H. M., Thijssen, J. M. and de Wilde, P. C. M.: influence of histochemical preparation on acoustic parameters of liver tissue: a 5-MHz study, 879

van der Steen, A. F. W., Rijsterborgh, H., Mastik, F., Lancée, C. T., van Hoorn, W. M. and Bom, N.: influence of attenuation on measurements of ultrasonic myocardial integrated backscatter during cardiac cycle (an *in vitro* study), 869

Stewart, P. A., see Huisman, T. W. A.

Stijnen, T., see van der Mooren, K.

Stones
analysis and classification of secondary sounds from the disintegration of kidney stones with acoustic shock waves (Olsson), 491
on the mechanism of kidney stone disintegration by acoustic shock waves (Holmer), 479
the mechanisms of stone disintegration by shock waves (Sass), 239

Streaming
a new ultrasonic method for fluid property measurements (Dymling), 497
Suhr, D., Brümmer, F. and Hülser, D. F.: cavitation-generated free radicals during shock wave exposure: investigation with cell-free solutions and suspended cells, 761
Sullivan, J. M., see Siddiqi, T. A.
Sundström, N., Börjesson, P. O., Holmer, N.-G., Olsson, L. and Persson, H. W.: registration of surface structures using airborne focused ultrasound, 513

Superoxide dismutase
cavitation-generated free radicals during shock wave exposure: investigation with cell-free solutions and suspended cells (Suhr), 761

Surgery
the mechanisms of stone disintegration by shock waves (Sass), 239

Synergism
synergism between hyperthermia, ultrasound and gamma irradiation (Loverock), 607

T

Takayasu's arteritis
carotid lesions detected by B-mode ultrasonography in Takayasu's arteritis: "macaroni sign" as an indicator of the disease (Maeda), 695
Tamura, T., Cobbold, R. S. C. and Johnston, K. W.: quantitative study of steady flow using color Doppler ultrasound, 595
Tanaka, M., see Saijo, Y.

Target detectability
ultimate limits in ultrasonic imaging resolution (Harris), 547
what might echography learn from imaging science? (Hill), 559
Teeuwen, C., see Legemate, D. A.

Temperature elevation
estimation of transient temperature elevation in lithotripsy and in ultrasonography (Filipczynski), 715
in utero measurement of ultrasonically induced fetal mouse temperature increases (Carnes), 373
the threshold for thermally significant cavitation in dog's thigh muscle *in vivo* (Hynynen), 157

Temporal effects
ultrasonic cavitation indirectly induces single strand breaks in DNA of viable cells *in vitro* by the action of residual hydrogen peroxide (Miller), 729
variability of quantitative echographic parameters of the liver: intra- and inter-individual spread, temporal- and age-related effects (Hartman), 857
Tessler, F. N. and Kimme-Smith, C.: author's reply to "velocity estimation using duplex scanners," 195L; 199L

Texture analysis
echographic differentiation of histological types of intraocular melanoma (Thijssen), 127
what might echography learn from imaging science? (Hill), 559

Therapeutic ultrasound
early metabolic response to high-energy shock waves in a human tumor kidney xenograft monitored by ^{31}P magnetic resonance spectroscopy (Smits), 791
effect of ultrasound on axonal outgrowth in the sympathetic nervous system of the chick (Yip), 139
effect of ultrasound on regional blood flow in neonatal rats (Muscarella), 893
in utero measurement of ultrasonically induced fetal mouse temperature increases (Carnes), 373
lack of induced increase in sister chromatid exchanges in human lymphocytes exposed to *in vivo* therapeutic ultrasound (Miller), 81
synergism between hyperthermia, ultrasound and gamma irradiation (Loverock), 607
the mechanisms of stone disintegration by shock waves (Sass), 239
the threshold for thermally significant cavitation in dog's thigh muscle *in vivo* (Hynynen), 157
thresholds for premature ventricular contractions in frog hearts exposed to lithotripter fields (Dalecki), 341

Thermal effects
effect of ultrasound on regional blood flow in neonatal rats (Muscarella), 893
synergism between hyperthermia, ultrasound and gamma irradiation (Loverock), 607
the threshold for thermally significant cavitation in dog's thigh muscle *in vivo* (Hynynen), 157

Thijssen, J. M., Verbeek, A. M., Romijn, R. L., de Wolff-Rouendaal, D. and Oosterhuis, J. A.: echographic differentiation of histological types of intraocular melanoma, 127
Thijssen, J. M., see Hartman, P. C.
Thijssen, J. M., see van der Steen, A. F. W.
Thomas, R. M., see Miller, D. L.
Thomas, R. M., see Miller, D. L.
Thomas, R. M., see Miller, D. L.

Thoracic aorta
assessment of a potentially noninvasive method for monitoring aortic blood flow in children (Lavandier), 107

Tissue characterisation
angle-dependent backscatter from the arterial wall (de Kroon), 121
applications of mixture laws for predicting the compositions of tissue phantoms (Jiang), 829
combined reflection and transmission ultrasound imaging (Green), 283
continuous-wave and pulsed Doppler studies of the breast: clinical results and effect of transducer frequency (Madjar), 31
echographic differentiation of histological types of intraocular melanoma (Thijssen), 127
identifying acoustic scattering sources in normal renal parenchyma from the anisotropy in acoustic properties (Insana), 613

measurement of blood perfusion in tissue using Doppler ultrasound (Dymling), 433
measurement of the ultrasonic properties of vascular tissues and blood from 35–65 MHz (Lockwood), 653
pulse-echo ultrasound speed measurements: progress and prospects (Robinson), 633
the relative contributions of myocardial wall thickness and ischemia to ultrasonic myocardial integrated backscatter during experimental ischemia (Rijsterborgh), 41
the ultrasonic properties of gastric cancer tissues obtained with a scanning acoustic microscope system (Saijo), 709
ultrasound properties of liver with and without particulate contrast agents (Tuthill), 231
what might echography learn from imaging science? (Hill), 559

Tissue effects
effect of ultrasound on regional blood flow in neonatal rats (Muscarella), 893
thresholds for premature ventricular contractions in frog hearts exposed to lithotripter fields (Dalecki), 341
ultimate limits in ultrasonic imaging resolution (Harris), 547

Tissue properties
ultimate limits in ultrasonic imaging resolution (Harris), 547

Toxicity
absence of mutagenic effects of continuous and pulsed ultrasound in cultured (A_L) human-hamster hybrid cells (Ritenour), 921

Transcranial Doppler
evaluation of cerebral blood flow in rabbits with transcranial Doppler sonography: first results (Tranquart), 815
evaluation of internal carotid artery stenosis by transcranial Doppler ultrasonography and oculopneumoplethysmography (Kelly), 577

Transducer
angle-dependent backscatter from the arterial wall (de Kroon), 121
combined reflection and transmission ultrasound imaging (Green), 283
measurements of ultrasonic fields with optical diffraction tomography (Holm), 505
pulse-echo imaging using a nondiffracting beam transducer (Lu), 265
registration of surface structures using airborne focused ultrasound (Sundström), 513
two-dimensional airborne ultrasound real-time linear array scanner—applied to screening for scoliosis (Mauritzson), 519

Transient thermal technique
absorption in liver at the focus of an ultrasonic shock wave field (Fry), 65

Transients
analysis and classification of secondary sounds from the disintegration of kidney stones with acoustic shock waves (Olsson), 491

Transmission
combined reflection and transmission ultrasound imaging (Green), 283

Transvaginal sonography
transvaginal sonography and abnormal ovarian appearance in menstrual cycle disturbances (Pache), 589

Tranquart, F., Berson, M., Bodard, S., Roncin, A. and Pourcelot, L.: evaluation of cerebral blood flow in rabbits with transcranial Doppler sonography: first results, 815
Trauner, E. J., see Fry, F. J.
Tuma, R. F., see Muscarella, L. F.

Tumors
continuous-wave and pulsed Doppler studies of the breast: clinical results and effect of transducer frequency (Madjar), 31
early metabolic response to high-energy shock waves in a human tumor kidney xenograft monitored by ^{31}P magnetic resonance spectroscopy (Smits), 791

Turbulence
change in amplitude distributions of Doppler spectrograms recorded below the aortic valve in patients with a valvular aortic stenosis (Cloutier), 667
quantitative study of steady flow using color Doppler ultrasound (Tamura), 595

Tuthill, P. A., Baggs, R. B., Violante, M. R. and Parker, K. J.: ultrasound properties of liver with and without particulate contrast agents, 231

U

Ueno, A., see Ritenour, E. R.

Ultimate limits
ultimate limits in ultrasonic imaging resolution (Harris), 547

Ultrasound
a measurement system for continuous-wave ultrasound fields (Persson), 501
a new ultrasonic method for fluid property measurements (Dymling), 497
absence of mutagenic effects of continuous and pulsed ultrasound in cultured (A_L) human-hamster hybrid cells (Ritenour), 921
absorption in liver at the focus of an ultrasonic shock wave field (Fry), 65
accuracy of velocity and shear rate measurements using pulsed Doppler ultrasound: a comparison of signal analysis techniques (Markou), 803
adaptive estimation of the mean frequency of a Doppler signal from short data windows (Herment), 901
an investigation of simulated umbilical artery Doppler waveforms. I. The effect of three physical parameters on the maximum frequency envelope and on pulsatility index (Hoskins), 7
an investigation of simulated umbilical artery Doppler waveforms. II. A comparison of three Doppler waveform quality indices (Hoskins), 23
an investigation of simulated umbilical artery Doppler waveforms. III. The effect of noise reduction algorithms on the maximum frequency envelope and on the pulsatility index (Hoskins), 703
analysis and classification of secondary sounds from the disintegration of kidney stones with acoustic shock waves (Olsson), 491
angle-dependent backscatter from the arterial wall (de Kroon), 121
aortic diameter pulse waves and blood flow velocity in the small, for gestational age, fetus (Stale), 471

applications of mixture laws for predicting the compositions of tissue phantoms (Jiang), 829
assessment of a potentially noninvasive method for monitoring aortic blood flow in children (Lavandier), 107
author's reply to "velocity estimation using duplex scanners," 195L (Tessler), 199L
calculation of pulse-wave velocity using cross correlation—effects of reflexes in the arterial tree (Benthin), 461
carotid lesions detected by B-mode ultrasonography in Takayasu's arteritis: "macaroni sign" as an indicator of the disease (Maeda), 695
cavitation-generated free radicals during shock wave exposure: investigation with cell-free solutions and suspended cells (Suhr), 761
change in amplitude distributions of Doppler spectrograms recorded below the aortic valve in patients with a valvular aortic stenosis (Cloutier), 667
clinical trial of umbilical artery Doppler waveform quality indices (Hoskins), 777
combined reflection and transmission ultrasound imaging (Green), 283
comparison of four different Doppler instruments used to measure linear and volumetric cardiac output: a study of reproducibility and agreement (Mayo), 347
computer analysis and pattern recognition of Doppler blood flow spectra for disease classification in the lower limb arteries (Allard), 211
continuous-wave and pulsed Doppler studies of the breast: clinical results and effect of transducer frequency (Madjar), 31
cyclic changes of blood echogenicity in high-frequency ultrasound (de Kroon), 723
Doppler flow velocity waveforms in the fetal cardiac outflow tract: reproducibility of waveform recording and analysis (Groenenberg), 583
duplex Doppler sonography of the umbilical arteries: predictive value in IUGR and correlation with birth weight (Worrell), 207
early echocardiography (Edler), 425
early metabolic response to high-energy shock waves in a human tumor kidney xenograft monitored by ^{31}P magnetic resonance spectroscopy (Smits), 791
echoencephalography and hyperostosis frontalis interna (White), 741L
echographic differentiation of histological types of intraocular melanoma (Thijssen), 127
effect of distal occlusions on the assessment of aorto-iliac pathology by analysis of Doppler spectra (Van Asten), 849
effect of fetal breathing movements on fetal cardiac hemodynamics (van der Mooren), 787
effect of maternal posture on the umbilical artery flow velocity waveform (van Katwijk), 683
effect of ultrasound on axonal outgrowth in the sympathetic nervous system of the chick (Yip), 139
effect of ultrasound on regional blood flow in neonatal rats (Muscarella), 893
effects of high-energy shock waves combined with biological response modifiers in different human kidney cancer xenografts (Oosterhof), 391
estimation of transient temperature elevation in lithotripsy and in ultrasonography (Filipczynski), 715
evaluation of cerebral blood flow in rabbits with transcranial Doppler sonography: first results (Tranquart), 815
evaluation of Doppler ultrasound for blood perfusion measurements (Eriksson), 445

evaluation of internal carotid artery stenosis by transcranial Doppler ultrasonography and oculopneumoplethysmography (Kelly), 577
flow velocity waveforms in the fetal inferior vena cava during the second half of normal pregnancy (Huisman), 679
identifying acoustic scattering sources in normal renal parenchyma from the anisotropy in acoustic properties (Insana), 613
in situ exposimetry: the ovarian ultrasound examination (Siddiqi), 257
in utero measurement of ultrasonically induced fetal mouse temperature increases (Carnes), 373
incorrect description of an ultrasonic beam (Kremkau), 411L
influence of attenuation on measurements of ultrasonic myocardial integrated backscatter during cardiac cycle (an *in vitro* study) (van der Steen), 869
influence of histochemical preparation on acoustic parameters of liver tissue: a 5-MHz study (van der Steen), 879
influence of various instrument settings on the flow information derived from the power mode (Jain), 49
influence of water conductivity on the efficacy and the reproducibility of electrohydraulic shock wave generation (Cathignol), 819
lack of induced increase in sister chromatid exchanges in human lymphocytes exposed to *in vivo* therapeutic ultrasound (Miller), 81
measurement of blood perfusion in tissue using Doppler ultrasound (Dymling), 433
measurement of intima-media thickness of common carotid arteries with high-resolution B-mode ultrasonography: inter- and intra-observer variability (Salonen), 225
measurement of the ultrasonic properties of vascular tissues and blood from 35–65 MHz (Lockwood), 653
measurements of ultrasonic fields with optical diffraction tomography (Holm), 505
mechanisms for hemolysis by ultrasonic cavitation in the rotating exposure system (Miller), 171
gauging the likelihood of cavitation from short-pulse, low-duty cycle diagnostic ultrasound (Apfel), 179
nonstationarity broadening in pulsed Doppler spectrum measurements (Fish), 147
on the mechanism of kidney stone disintegration by acoustic shock waves (Holmer), 479
phase cancellation: a cause of acoustical shadowing at the edges of curved surfaces in B-mode ultrasound images (Rubin), 85
prediction of *in situ* exposure to ultrasound: a proposed standard experimental method (Preston), 333
prediction of *in situ* exposure to ultrasound: an acoustical attenuation method (Preston), 317
prenatal diagnosis, management and outcome of fetal uretero-pelvic junction obstruction (Bosman), 117
pulse-echo imaging using a nondiffracting beam transducer (Lu), 265
pulse-echo ultrasound speed measurements: progress and prospects (Robinson), 633
pulsed ultrasound and neoplastic transformation *in vitro* (Harrison), 627
pulsed ultrasound and the hyperbarically exposed mouse fetus (Child), 367
quantitative study of steady flow using color Doppler ultrasound (Tamura), 595
regions in the B-mode image of a cylinder where the location of a point reflector is changed by sound speed variation (Soetanto), 355

registration of surface structures using airborne focused ultrasound (Sundström), 513
reversible biochemical changes in the developing rat central nervous system following ultrasound exposure (Margulies), 383
robust electromagnetic probe for the monitoring of lithotriptor output (Pye), 931
single strand breaks in CHO cell DNA induced by ultrasonic cavitation *in vitro* (Miller), 401
sonographic, clinical and genetic aspects of prenatal diagnosis of cystic kidney disease (Reuss), 687
sonoluminescence in water and agar gels during irradiation with 0.75 MHz continuous-wave ultrasound (Daniels), 297
spectral analysis criteria in duplex scanning of aortoiliac and femoropopliteal arterial disease (Legemate), 769
spectral composition of Doppler signals (Hoeks), 751
statistical uncertainty in ultrasonic backscatter and attenuation coefficients determined with a reference phantom (Yao), 187
synergism between hyperthermia, ultrasound and gamma irradiation (Loverock), 607
the mechanisms of stone disintegration by shock waves (Sass), 239
the relative contributions of myocardial wall thickness and ischemia to ultrasonic myocardial integrated backscatter during experimental ischemia (Rijsterborgh), 41
the threshold for thermally significant cavitation in dog's thigh muscle *in vivo* (Hynynen), 157
the ultrasonic properties of gastric cancer tissues obtained with a scanning acoustic microscope system (Saijo), 709
the use of frequency mixing to distinguish size distributions of gas-filled micropores (Quain), 71
the use of ink jets in ultrasound registrations (Johansson), 529
theoretical predictions of the acoustic pressure generated by a shock wave lithotripter (Coleman), 245
thresholds for premature ventricular contractions in frog hearts exposed to lithotripter fields (Dalecki), 341
transvaginal sonography and abnormal ovarian appearance in menstrual cycle disturbances (Pache), 589
two-dimensional airborne ultrasound real-time linear array scanner—applied to screening for scoliosis (Mauritzson), 519
ultimate limits in ultrasonic imaging resolution (Harris), 547
ultrasonic cavitation indirectly induces single strand breaks in DNA of viable cells *in vitro* by the action of residual hydrogen peroxide (Miller), 729
ultrasound effects on cell proliferation and migration of chick motoneurons (Yip), 55
ultrasound properties of liver with and without particulate contrast agents (Tuthill), 231
variability of quantitative echographic parameters of the liver: intra- and inter-individual spread, temporal- and age-related effects (Hartman), 857
velocity estimation using duplex scanners (Hoskins), 195L
volume measurement by ultrasonic transverse or sagittal cross-sectional scanning (Basset), 291
waveform pattern recognition—a new semiquantitative method for the analysis of fetal aortic and umbilical artery blood flow velocity recorded by Doppler ultrasound (Malcus), 453
what might echography learn from imaging science? (Hill), 559

Umbilical artery
an investigation of simulated umbilical artery Doppler waveforms. I. The effect of three physical parameters on the maximum frequency envelope and on pulsatility index (Hoskins), 7
an investigation of simulated umbilical artery Doppler waveforms. II. A comparison of three Doppler waveform quality indices (Hoskins), 23
an investigation of simulated umbilical artery Doppler waveforms. III. The effect of noise reduction algorithms on the maximum frequency envelope and on the pulsatility index (Hoskins), 703
clinical trial of umbilical artery Doppler waveform quality indices (Hoskins), 777
duplex Doppler sonography of the umbilical arteries: predictive value in IUGR and correlation with birth weight (Worrell), 207
effect of maternal posture on the umbilical artery flow velocity waveform (van Katwijk), 683
waveform pattern recognition—a new semiquantitative method for the analysis of fetal aortic and umbilical artery blood flow velocity recorded by Doppler ultrasound (Malcus), 453

Utero-pelvic junction obstruction
prenatal diagnosis, management and outcome of fetal uretero-pelvic junction obstruction (Bosman), 117

V

Vaginal sonography
transvaginal sonography and abnormal ovarian appearance in menstrual cycle disturbances (Pache), 589

Van Asten, W. N. J. C., Beijneveld, W. J., van Lier, H. J. J., Wijn, P. F. F. and Skotnicki, S. H.: effect of distal occlusions on the assessment of aorto-iliac pathology by analysis of Doppler spectra, 849

Variance
quantitative study of steady flow using color Doppler ultrasound (Tamura), 595

Vasthare, U., see Muscarella, L. F.

Velocity mode
influence of various instrument settings on the flow information derived from the power mode (Jain), 49

Velocity profile
accuracy of velocity and shear rate measurements using pulsed Doppler ultrasound: a comparison of signal analysis techniques (Markou), 803
spectral composition of Doppler signals (Hoeks), 751

Verbeek, A. M., see Thijssen, J. M.
Verdouw, P. D., see Rijsterborgh, H.
Violante, M. R., see Tuthill, P. A.

Viscosity
a new ultrasonic method for fluid property measurements (Dymling), 497

Vision
what might echography learn from imaging science? (Hill), 559

Visual perception
what might echography learn from imaging science? (Hill), 559

Volume flow
assessment of a potentially noninvasive method for monitoring aortic blood flow in children (Lavandier), 107

Volume measurement
volume measurement by ultrasonic transverse or sagittal cross-sectional scanning (Basset), 291

Vortex
quantitative study of steady flow using color Doppler ultrasound (Tamura), 595

W

Waag, R. C., see Quain, R. M.
van der Wal, L. F., see de Kroon, M. G. M.
Waldren, C. A., see Ritenour, E. R.

Wall motion
assessment of a potentially noninvasive method for monitoring aortic blood flow in children (Lavandier), 107

Wall thickness
influence of attenuation on measurements of ultrasonic myocardial integrated backscatter during cardiac cycle (an *in vitro* study) (van der Steen), 869
measurement of intima-media thickness of common carotid arteries with high-resolution B-mode ultrasonography: inter- and intra-observer variability (Salonen), 225
the relative contributions of myocardial wall thickness and ischemia to ultrasonic myocardial integrated backscatter during experimental ischemia (Rijsterborgh), 41

Waveform quality index
clinical trial of umbilical artery Doppler waveform quality indices (Hoskins), 777

Waveforms
the threshold for thermally significant cavitation in dog's thigh muscle *in vivo* (Hynynen), 157

Way, J. S., see Margulies, N.
Webb, S., see Hill, C. R.
Wells, P. N. T., see Harris, R. A.
White, D. N. and Saunders, F. W.: echoencephalography and hyperostosis frontalis interna, 741L
Whitehurst, T. K., see Green, P. S.
Wijn, P. F. F., see Van Asten, W. N. J. C.
de Wilde, P. C. M., see van der Steen, A. F. W.
Williams, A. R., see Miller, D. L.
Willner, S., see Mauritzson, L.
Wilson, L. S., see Robinson, D. E.

Windows
nonstationarity broadening in pulsed Doppler spectrum measurements (Fish), 147

Wladimiroff, J. W., see Bosman, G.
Wladimiroff, J. W., see Groenenberg, I. A. L.
Wladimiroff, J. W., see Huisman, T. W. A.
Wladimiroff, J. W., see van Katwijk, C.
Wladimiroff, J. W., see van der Mooren, K.
Wladimiroff, J. W., see Pache, T. D.
Wladimiroff, J. W., see Reuss, A.
Wojcik, J., see Filipczynski, L.
de Wolff-Rouendaal, D., see Thijssen, J. M.
Worrell, J. A., Fliescher, A. C., Drolshagen, L. F., Durmon, G. R. and Shah, D. M.: duplex Doppler sonography of the umbilical arteries: predictive value in IUGR and correlation with birth weight, 207

X

X-rays
pulsed ultrasound and neoplastic transformation *in vitro* (Harrison), 627

Xenografts
effects of high-energy shock waves combined with biological response modifiers in different human kidney cancer xenografts (Oosterhof), 391

Y

Yao, L. X., Zagzebski, J. A. and Madsen, E. L.: statistical uncertainty in ultrasonic backscatter and attenuation coefficients determined with a reference phantom, 187
Yip, J. W., see Yip, Y. P.
Yip, J. W., see Yip, Y. P. L.
Yip, Y. P., Capriotti, C., Norbash, S. G., Rosenthal, M. S. and Yip, J. W.: ultrasound effects on cell proliferation and migration of chick motoneurons, 55
Yip, Y. P. L., Capriotti, C., Rosenthal, M. S., He, B. Q. and Yip, J. W.: effect of ultrasound on axonal outgrowth in the sympathetic nervous system of the chick, 139
Yoganathan, A. P., see Jain, S. P.
Yoneda, S., see Maeda, H.

Young's modulus
calculation of pulse-wave velocity using cross correlation—effects of reflexes in the arterial tree (Benthin), 461

Z

Zagzebski, J. A., see Yao, L. X.
Zeqiri, B., see Preston, R. C.
Zeqiri, B., see Preston, R. C.
Ziskin, M. C., see Margulies, N.
Ziskin, M. C., see Muscarella, L. F.